Pathway analysis using (13) C-glycerol and other carbon tracers reveals a bipartite metabolism of Legionella pneumophila

Häuslein, Ina ; Manske, Christian ; Goebel, Werner ; Eisenreich, Wolfgang ; Hilbi, Hubert

Abstract: Amino acids represent the prime carbon and energy source for Legionella pneumophila, a facultative intracellular pathogen, which can cause a life-threatening pneumonia termed Legionnaires' disease. Genome, transcriptome and proteome studies indicate that L. pneumophila also utilizes carbon substrates other than amino acids. We show here that glycerol promotes intracellular replication of L. pneumophila in amoeba or macrophages (but not extracellular growth) dependent on glycerol-3-phosphate dehydrogenase, GlpD. An L. pneumophila mutant strain lacking glpD was outcompeted by wild-type bacteria upon co-infection of amoeba, indicating an important role of glycerol during infection. Isotopologue profiling studies using (13) C-labelled substrates were performed in a novel minimal defined medium, MDM, comprising essential amino acids, proline and phenylalanine. In MDM, L. pneumophila utilized (13) C-labelled glycerol or glucose predominantly for gluconeogenesis and the pentose phosphate pathway, while the amino acid serine was used for energy generation via the citrate cycle. Similar results were obtained for L. pneumophila growing intracellularly in amoeba fed with (13) C-labelled glycerol, glucose or serine. Collectively, these results reveal a bipartite metabolism of L. pneumophila, where glycerol and carbohydrates like glucose are mainly fed into anabolic processes, while serine serves as major energy supply.

DOI: https://doi.org/10.1111/mmi.13313

Pathway analysis using ^{13}C-glycerol and other carbon tracers reveals a bipartite metabolism of *Legionella pneumophila*

Ina Häuslein[1#], Christian Manske[2#], Werner Goebel[2], Wolfgang Eisenreich[1]* and Hubert Hilbi[2,3]*

[1] *Lehrstuhl für Biochemie, Technische Universität München, Munich, Germany*

[2] *Max von Pettenkofer Institut, Ludwig-Maximilians Universität, Munich, Germany*

[3] *Institute of Medical Microbiology, University of Zürich, Switzerland*

[#] These authors contributed equally to the work.

Running title: Bipartite metabolism of *L. pneumophila*

Key words: amoeba, *Legionella*, isotopologue profiling, macrophage, metabolism, nutrition, pathogen vacuole, type IV secretion

***Address correspondence to Wolfgang Eisenreich, Lichtenbergstrasse 4, 85747 Garching, Germany, Tel +49-89-289-13336, Fax +49-89-289-13363, e-mail wolfgang.eisenreich@ch.tum.de; or Hubert Hilbi, Gloriastrasse 30, 8006 Zürich, Switzerland, Tel +41-44-634-2650, Fax +41-44-634-4906, e-mail hilbi@imm.uzh.ch

This article has been accepted for publication and undergone full peer review but has not been through the copyediting, typesetting, pagination and proofreading process which may lead to differences between this version and the Version of Record. Please cite this article as an 'Accepted Article', doi: 10.1111/mmi.13313

Summary

Amino acids represent the prime carbon and energy source for *Legionella pneumophila*, a facultative intracellular pathogen, which can cause a life-threatening pneumonia termed Legionnaires' disease. Genome, transcriptome and proteome studies indicate that *L. pneumophila* also utilizes carbon substrates other than amino acids. We show here that glycerol promotes intracellular replication of *L. pneumophila* in amoeba or macrophages (but not extracellular growth) dependent on glycerol-3-phosphate dehydrogenase, GlpD. An *L. pneumophila* mutant strain lacking *glpD* was outcompeted by wild-type bacteria upon co-infection of amoeba, indicating an important role of glycerol during infection. Isotopologue profiling studies using ^{13}C-labelled substrates were performed in a novel minimal defined medium, MDM, comprising essential amino acids, proline and phenylalanine. In MDM, *L. pneumophila* utilized ^{13}C-labelled glycerol or glucose predominantly for gluconeogenesis and the pentose phosphate pathway, while the amino acid serine was used for energy generation via the citrate cycle. Similar results were obtained for *L. pneumophila* growing intracellularly in amoeba fed with ^{13}C-labelled glycerol, glucose or serine. Collectively, these results reveal a bipartite metabolism of *L. pneumophila*, where glycerol and carbohydrates like glucose are mainly fed into anabolic processes, while serine serves as major energy supply.

Introduction

Legionella pneumophila is a facultative intracellular pathogen that can replicate in a wide range of protozoan host cells, including *Acanthamoeba* and *Hartmanella* spp. (Steinert & Heuner, 2005, Hoffmann *et al.*, 2014b). *L. pneumophila* can also infect humans, as the bacteria are able to replicate within alveolar macrophages, causing a severe pneumonia called Legionnaires' disease. The pathogen adopts a biphasic life style, which comprises a replicative and a transmissive (virulent) stage and is regulated by the growth phase (Molofsky & Swanson, 2004). While exponentially growing bacteria repress transmissive features such as virulence, motility and stress resistance, bacteria in post-exponential phase induce these traits (Byrne & Swanson, 1998, Brüggemann *et al.*, 2006, Faucher *et al.*, 2011).

The mechanism underlying intracellular survival of the bacteria in different phagocytic host cells seem to be evolutionarily conserved (Hoffmann *et al.*, 2014b) and includes the formation of a replication-permissive compartment termed the *Legionella*-containing vacuole (LCV). The LCV acquires components of early and late endosomes, mitochondria, the endoplasmic reticulum as well as ribosomes, yet it avoids fusion with lysosomes and concomitant degradation (Hubber & Roy, 2010, Isberg *et al.*, 2009, Hilbi & Haas, 2012, Sherwood & Roy, 2013, Hoffmann *et al.*, 2014a). To establish its replicative intracellular niche, *L. pneumophila* uses the Icm/Dot type IV secretion system (T4SS), which translocates a plethora of "effector" proteins into the host cell. These effectors target central eukaryotic pathways like endocytic, secretory or retrograde vesicle trafficking and modulate host factors such as small GTPases, phosphoinositide lipids or phytate (Finsel & Hilbi, 2015, Finsel *et al.*, 2013, Haneburger & Hilbi, 2013, Rothmeier *et al.*, 2013, Weber *et al.*, 2014).

While the mechanisms of intracellular survival of *L. pneumophila* are rather well studied, the carbon metabolism of intracellular and extracellular bacteria is still poorly understood. Early *in vitro* studies of *L. pneumophila* metabolism showed a preference for amino acids as main source of carbon and energy, and auxotrophy for several amino acids including arginine,

cysteine, isoleucine, leucine, methionine, serine and threonine was reported. (Pine *et al.*, 1979, Ristroph *et al.*, 1981, Tesh & Miller, 1981, Tesh *et al.*, 1983). The *L. pneumophila* genome encodes various amino acid transporters and proteases, which is further highlighting the importance of amino acids for the bacterial metabolism (Cazalet *et al.*, 2004, Chien *et al.*, 2004). The identification of the phagosomal transporter family (Pht) revealed a role of amino acid metabolism during intracellular growth, as *L. pneumophila* mutants lacking the threonine transporter PhtA, the valine transporter PhtJ or the thymidine transporters PhtC and PhtD no longer grow inside macrophages (Sauer *et al.*, 2005, Chen *et al.*, 2008, Fonseca *et al.*, 2014). Also, Icm/Dot-translocated effectors seem to promote the usage of amino acids during intracellular growth. The *L. pneumophila* ubiquitin ligase AnkB highjacks host cell amino acid metabolism by exploiting the proteasome to create a pool of free amino acids within the host cell (Lomma *et al.*, 2010, Price *et al.*, 2009, Price *et al.*, 2011). Using host cell transporters, these amino acids can then be shuttled into the LCV. The eukaryotic neutral amino acid transporter SLC1A5, e. g., is upregulated in infected cells and essential for intracellular growth of *L. pneumophila* (Wieland *et al.*, 2005).

In addition to amino acids, *L. pneumophila* is also able to metabolize carbohydrates. This is reflected in the genomes of sequenced *Legionella* species, which encode complete Embden-Meyerhof-Parnas (EMP) and Entner-Doudoroff (ED) pathways, but only the non-oxidative part of the pentose phosphate pathway (PPP) (Chien *et al.*, 2004, D'Auria *et al.*, 2010, Cazalet *et al.*, 2010). This incomplete PPP lacking 6-phosphogluconate dehydrogenase suffices to catalyze the interconversion of sugars needed for cell wall biosynthesis, but does not yield $NADPH/H^+$. *L. pneumophila* mutants lacking different genes of the ED pathway are defective for intracellular growth in amoeba and mammalian cells, and wild-type bacteria indeed catabolize glucose via the ED pathway, as shown by transcriptome and proteome studies as well as by isotopologue profiling (Eylert *et al.*, 2010, Harada *et al.*, 2010, Schunder *et al.*, 2014, Hoffmann *et al.*, 2014b).

Isotopologue profiling is a powerful tool for metabolic studies and can give detailed insights into metabolic pathways and fluxes. The method is based upon ^{13}C-incorporation derived from labelled precursors that are metabolized by bacteria or eukaryotic cells. To this end, the overall ^{13}C-enrichment and the isotopologue composition in key metabolic products are determined, preferably using gas chromatography/mass spectrometry (GC/MS). This technique has been used for a range of bacteria, including *Listeria monocytogenes* (Gillmaier *et al.*, 2012), *Streptococcus pneumonia* (Hartel *et al.*, 2012), *Staphylococcus aureus* (Kriegeskorte *et al.*, 2014), *Campylobacter jejuni* (Vorwerk *et al.*, 2014) or *Xanthomonas campestris* (Schatschneider *et al.*, 2014).

Glycerol is an important carbon source for different intracellular pathogens, such as *L. monocytogenes* (Grubmüller *et al.*, 2014) or *Salmonella enterica* (Steeb *et al.*, 2013). Upon intracellular growth of *L. pneumophila* in macrophages, the expression of glycerol kinase (*lpg1414*, *glpK*) and glycerol-3-phosphate dehydrogenase (*glpD*) is highly upregulated (Faucher *et al.*, 2011), and early studies using a defined medium indicated that glycerol might also be metabolized by *L. pneumophila* (Tesh *et al.*, 1983). In this study, we analysed glycerol metabolism of extra- and intracellularly growing *L. pneumophila* using different growth assays, isotopologue profiling and a newly developed *Legionella* minimal growth medium. The use of [U-$^{13}C_3$]glycerol as a tracer indicated that the compound indeed serves as a nutrient for *L. pneumophila* and is predominantly metabolized via gluconeogenesis and the PPP. Furthermore, ^{13}C-incorporation into key metabolites of *L. pneumophila* growing either with [U-$^{13}C_3$]glycerol, [U-$^{13}C_6$]glucose or [U-$^{13}C_3$]serine revealed a bipartite metabolism, where glycerol and carbohydrates such as glucose are predominantly channelled into glycolysis, gluconeogenesis and the PPP, respectively, and hence used mainly for anabolic reactions, while especially serine is used effectively in the TCA cycle to deliver reducing equivalents for energy production in the electron transport chain.

Results

Designing a new chemically defined Legionella *growth medium*

In initial attempts, we used chemically defined medium (CDM) (Eylert *et al.*, 2010) modified from "Ristroph medium" (Ristroph *et al.*, 1981) to assess with different microbiological assays and by isotopologue profiling the effect of glycerol on extracellular growth of *L. pneumophila* strains (Table S1). However, under the conditions used no significant ^{13}C-enrichment was detectable in any metabolite (data not shown). To develop a new *Legionella* growth medium, we minimized the carbon sources in CDM as far as possible but did not alter salt composition and iron concentration. A medium that contained only essential amino acids (arginine, cysteine, isoleucine, leucine, methionine, serine, threonine, valine) was not suitable, as *L. pneumophila* did not replicate in this medium anymore (data not shown).

Next, we depleted single non-essential amino acids from CDM. Depletion of histidine, lysine, proline, tryptophan and aspartate did not alter *L. pneumophila* growth compared to normal CDM (Figure S1A). CDM lacking serine did not support growth of *L. pneumophila*, highlighting the importance of serine for *Legionella* growth. Leaving out pairs of amino acids such as aspartate and histidine or aspartate and tryptophan yielded a medium that supported robust growth of *L. pneumophila* similar to CDM. Depletion of aspartate and lysine or aspartate and proline resulted in reduced growth compared to CDM. We then used a medium, lacking all amino acids that had no significant influence on *L. pneumophila* growth, namely histidine, aspartate, tryptophan, lysine and glutamate. The medium still contained proline, as depletion of this amino acid significantly reduced growth. In this medium, *L. pneumophila* did not reach optical densities as high as in CDM (Figure S1B), but the bacteria did reach stationary growth phase as judged by the production of the brown pigment, motility and shape of the bacteria (data not shown). Finally, the omission of the aromatic amino acid tyrosine from CDM had no effect on growth, but leaving out phenylalanine or both, phenylalanine and tyrosine, significantly reduced growth (Figure S1C). Tyrosine can be directly synthesised

from phenylalanine in the reaction catalyzed by phenylalanine hydroxylase (*phhA*), explaining why depletion of tyrosine had no growth effect and why phenylalanine is more required in the medium than tyrosine. In summary, the optimized new medium termed minimal defined medium (MDM) was composed of CDM lacking aspartate, glutamate, histidine, lysine, tryptophan and tyrosine (Table S2).

Glycerol promotes intracellular growth of L. pneumophila

To analyse the role of glycerol in the metabolism of *L. pneumophila*, we constructed the deletion mutant Δ*glpD*, lacking the glycerol-3-phosphate dehydrogenase GlpD (strain CM01, Table S1). The growth of *L. pneumophila* Δ*glpD* was indistinguishable from wild-type bacteria in AYE broth (data not shown) and slightly reduced in CDM (Figure 1A) or MDM (Figure 1B). The addition of glycerol had no effect on extracellular growth of *L. pneumophila* in AYE (data not shown), CDM (Figure 1A) or MDM (Figure 1B). Moreover, the addition of 10 mM or 20 mM glycerol-3-phosphate did not affect the growth of *L. pneumophila* in MDM, but 50 mM of the compound decreased the growth of wild-type or Δ*glpD* mutant bacteria (Figure 1C, Figure S2). Thus, under the conditions tested, neither glycerol nor glycerol-3-phosphate promotes the extracellular growth of *L. pneumophila* in different media.

The effect of glycerol on intracellular growth of *L. pneumophila* was determined by fluorescence-based assays and colony-forming units (cfu). As expression of *glpD* was upregulated upon growth in macrophages (Faucher *et al.*, 2011), we used RAW 264.7 macrophages to analyse intracellular growth. The addition of 50 mM glycerol 4 h post infection increased the cell numbers of wild-type *L. pneumophila* in stationary growth phase (Figure 1D, Figure 1E). The Δ*glpD* mutant strain grew intracellularly like wild-type *L. pneumophila*, but glycerol did not promote growth. The mutant phenotype was complemented by providing *glpD* on a plasmid (Figure 1E). Furthermore, glycerol promoted the growth of *L. pneumophila* not only in macrophages, but also in *A. castellanii* (Figure 1F). Interestingly,

upon co-infection of *A. castellanii* with *L. pneumophila* wild-type and Δ*glpD*, the mutant was outcompeted within 3-6 days, indicating that lack of *glpD* reduced intracellular growth and/or persistence in presence of the amoeba (Figure 1G, Figure S3). The competition defect was complemented by providing *glpD* on a plasmid (Figure 1H). Taken together, glycerol does not have an effect on extracellular growth of *L. pneumophila* in complex or defined minimal media, but promotes intracellular growth in macrophages and amoeba.

Glycerol metabolism of L. pneumophila *growing in MDM*

In order to further study glycerol metabolism of *L. pneumophila* we used isotopologue profiling, which is a sensitive method to monitor also minor carbon flows. Initial experiments with *L. pneumophila* grown in CDM and fed with [U-$^{13}C_3$]glycerol did not yield significant ^{13}C-enrichments in any metabolite (data not shown). However, isotopologue measurements of *L. pneumophila* growing in the newly developed MDM revealed that glycerol was indeed metabolized (Figure 2A). Under the experimental conditions used, ^{13}C-label derived from [U-$^{13}C_3$]glycerol was primarily found in histidine (3.01%), a marker of the PPP (through its precursor phosphoribosyl pyrophosphate, PRPP), and in mannose (5.75%), a valid reporter metabolite for gluconeogenesis. To a small amount, ^{13}C-enrichment was also detectable in lactate (0.97%) and in DAP (0.74%) as well as in malate (0.70%), 3-hydroxybutyric acid (0.61%), stearic acid (0.60%) and glutamate (0.55%). With the exception of lactate (0.71%), incorporation of ^{13}C-label was not detected in these metabolites using the mutant strain Δ*glpD* (Figure 2A). These results provided a strong indication that glycerol was metabolized by *L. pneumophila* wild-type dependent on the glycerol-3-phosphate dehydrogenase GlpD.

The isotopologue profile of mannose mainly displayed M+3 (i.e. specimens that carry 3 ^{13}C-atoms) and to minor extent M+6 (i.e. specimens that carry 6 ^{13}C-atoms), suggesting that glycerol was metabolized via gluconeogenesis to yield hexoses (Figure 2B). Histidine as a marker amino acid for the PPP, showed mainly M+2 and M+3 labelling. This pattern supports

the notion that the gluconeogenetic pathway is active. Here, fully labelled glyceraldehyde-3-phosphate or dihydroxyacetone-phosphate derived from [U-$^{13}C_3$]glycerol is used for the synthesis of fructose-1,6-bisphosphate and fructose-6-phosphate, the direct precursor of mannose-6-phosphate. Due to one or two ^{13}C-precursors used for the assembly, these hexoses are M+3 or M+6 labelled. Subsequently, C_5-sugars are built in transketolase reactions in the PPP, yielding M+3 and M+2 labels of C_5-sugars, such as PRPP. This pentose is a precursor unit in histidine biosynthesis, in agreement with the observed labelling pattern of histidine (Figure 2B). Transketolase reactions also lead to M+3 or M+1 label in erythrose-4-phosphate, M+1 supposedly at position C-1. The single label in mannose, which was detected in minor amounts, is then the result of a transketolase reaction that transfers the M+1 label at position C-1 onto xylulose-5-phosphate (Figure 2B).

No ^{13}C-label was detected in essential amino acids (isoleucine, leucine, serine, valine) and in most of the amino acids derived from the TCA cycle (alanine, aspartate, lysine, proline) or TCA cycle intermediates (succinate, fumarate, citrate) (Figure 2A). Collectively, these results implied that glycerol is metabolized by the TCA cycle only to a minor extent and instead is used predominantly for gluconeogenesis and PPP. Notably, lactate was the only metabolite that showed some ^{13}C-enrichment in the Δ*glpD* mutant strain (0.71%, Figure 2A). The labelling pattern for lactate was identical in wild-type *L. pneumophila* and the Δ*glpD* mutant and showed only completely labelled isotopologues (M+3, Figure 2B). ^{13}C-Excess and isotopologue profiles of endpoint experiments are shown in Table S3.

Time-dependent usage of glycerol by L. pneumophila

For an in-depth analysis of the determinants of glycerol metabolism by *L. pneumophila*, we assessed glycerol utilization in a time-dependent manner in comparison to other carbon sources used by the bacteria. To this end, we chose serine and glucose, as it is known that both compounds are metabolized by *L. pneumophila in vitro* (Eylert *et al.*, 2010). To compare

the metabolism of these substrates in parallel, we added 11 mM glucose and 50 mM glycerol to MDM, which already contained 6 mM serine as an essential amino acid. This adjusted medium was termed "carbon-enriched minimal defined medium" (CE MDM). In the following time series experiments, one of these substrates was added as ^{13}C-labelled compound. After 12 h, 24 h, 36 h or 48 h of growth, the bacteria were harvested. ^{13}C-Enrichment and isotopologue pattern of protein-derived amino acids, mannose and DAP (both compounds presumably produced by cell wall hydrolysis), 3-hydroxybutyrate (named polyhydroxybutyrate (PHB) in the following, since presumably derived from PHB hydrolysis) and other polar metabolites, as well as fatty acids were analysed as described above. The time points were chosen to represent early exponential (12 h), exponential (24 h), late exponential (36 h) and stationary (48 h) growth phase of *L. pneumophila* growing in MDM (Figure 1B). ^{13}C-Excess and isotopologue profiles of all time-series experiments are documented in Table S4.

The time-series experiment with *L. pneumophila* grown in CE MDM with [U-$^{13}C_3$]glycerol as precursor yielded significant enrichments especially in histidine (3.00% after 48 h) and mannose (4.51% after 48 h) (Figure 3A, D). Although this medium contained glucose as possible carbon source besides glycerol, the ^{13}C-enrichment in histidine was similar compared to the experiment in MDM after 48 h (Figure 2A). The ^{13}C-abundance in mannose was decreased by only approximately 20%, suggesting that glucose had only a minor influence on the metabolism of glycerol. Additionally, ^{13}C-enrichments were also found to a minor extent in alanine (0.61%), aspartate (0.49%), glutamate (0.77%), DAP (0.80%), PHB (0.52%), lactate (1.44%) and malate (0.55%) after 48 h of growth. Notably, significant enrichment in any metabolite was only detectable after 36 h incubation, indicating that glycerol was only used in later stages of exponential growth and in the stationary growth phase (48 h), where the highest ^{13}C-abundances were measured. Furthermore, the isotopologue pattern in histidine, mannose and lactate were almost identical compared to their isotopologue pattern during

growth in MDM (Figure S4A), indicating that also in CE MDM glycerol was predominantly used for gluconeogenesis and PPP and only to a minor extent in the TCA cycle.

Similar to the time-series experiments with [U-$^{13}C_3$]glycerol, [U-$^{13}C_6$]glucose added as a supplement to the medium yielded the highest ^{13}C-enrichments in histidine and mannose (20.72% and 31.88% after 48 h). Additionally, several other metabolites were also significantly labelled when grown with ^{13}C-glucose, including alanine, aspartate, glutamate, lysine, proline, DAP, PHB, succinate, fumarate, palmitate and stearate (ranging from 4.26% to 1.38% overall excess after 48 h) (Figure 3B, Figure 3D). The isotopologue profile of histidine did not differ from labelling experiments with [U-$^{13}C_3$]glycerol and mainly showed M+2 and M+3. The label of mannose was primarily M+3 and M+6 (Figure S4B). This data confirmed that glucose was predominantly metabolized via the ED pathway (Eylert *et al.*, 2010, Harada *et al.*, 2010), gluconeogenesis and the PPP, and was also used to a minor extent via the TCA cycle to yield precursors for amino acids and fatty acids. Different to glycerol, glucose was moderately used as a carbon source already at earlier stages of *L. pneumophila* growth (significant enrichment after 12 h). Intermediates of the TCA cycle (succinate, fumarate, malate) and amino acids derived from the TCA cycle (aspartate, glutamate) were mainly M+1 and M+2 labelled (Figure S4B). The M+2 label is derived from fully labelled acetyl-CoA, while M+1 label could reflect the decarboxylation reaction of the α-ketoglutarate-dehydrogenase or multiple rounds of TCA cycle, where unlabelled acetyl-CoA is transferred onto labelled oxaloacetate. Besides histidine, alanine was the highest labelled amino acid (4.26%) with mainly M+3, which indicates that this compound was directly derived from fully labelled pyruvate presumably derived from reactions of the ED pathway as the major route of glucose metabolism in *L. pneumophila* (Eylert *et al.*, 2010, Harada *et al.*, 2010). Interestingly, lactate showed no significant ^{13}C-enrichment, thus differing from labelling experiments with glycerol.

To rule out that the metabolism of glycerol and glucose was mutually influenced by the presence of the other carbon substrate, we also performed time series experiments in MDM where either glycerol or glucose was added as ^{13}C-labelled precursor in absence of the other substrate. The change in setup resulted in no significant change in ^{13}C-incorporation and labelling pattern (data not shown), compared to time series experiments in CE MDM, where the metabolism of one labelled carbon source was analyzed in presence of the other, unlabelled substrate. These findings indicate that serine, glycerol and glucose are co-metabolized independently by *L. pneumophila*.

When incubated with [U-$^{13}C_3$]serine as precursor, ^{13}C-enrichment was detected in the same metabolites as in the time series experiment with labelled glucose. Additionally, also glycine was highly ^{13}C-enriched (28.58% after 24 h) (Figure 3C, Figure 3D). The isotopologue pattern of glycine showed that it was directly synthesised from serine, as it was almost completely M+2 labelled (Figure S4C). In difference to the above labelling experiments the overall ^{13}C-enrichment reached its peak already after 24 h and was dropping steadily afterwards. The ^{13}C-excess from significantly labelled amino acids, DAP and PHB after 24 h ranged between 91.61% in serine to 28.58% in glycine (serine > alanine > histidine > DAP > lysine > PHB > aspartate > glutamate > glycine). This shows that serine was very efficiently taken up from the medium and metabolized (Figure 3C). After 48 h of growth, also intermediates of the TCA cycle, fatty acids and mannose were highly labelled, ranging between 3.53% and 40.40% overall enrichment (Figure 3D). The high enrichment in alanine (74.60% after 24 h) and in amino acids derived from the TCA cycle could reflect that serine was mainly fed into the TCA cycle. This notion is in agreement with the high abundance of ^{13}C-label in succinate, fumarate and malate, as well as in fatty acids, which also indicates a high carbon flow into the TCA cycle. The isotopologue profile of palmitate and stearate mainly showed M+2, M+4, M+6, M+8, M+10 and M+12 labelling (Figure S4C). This fractional profile shows high carbon flux from serine to acetyl-CoA, which is then

incorporated as C2-building blocks into fatty acids. The profile was different in experiments with ^{13}C-glucose, where mostly M+2 labelling was detected in the isotopologue pattern of fatty acids, suggesting a lower flow of acetyl-CoA into fatty acid biosynthesis. Labelled acetyl-CoA derived from ^{13}C-labelled serine was also used for the synthesis of PHB and its precursor 3-hydroxybutyrate. The isotopologue pattern of both metabolites was identical (mostly M+2) and contained also a fraction of M+4 derived from the condensation of two fully labelled acetyl-CoA. Again, the profile was different from experiments with ^{13}C-glucose, where the M+4 fraction was not detectable (Figure S4B, Figure S4C).

Aspartate is synthesized from oxaloacetate which is either derived from the TCA cycle or directly by carboxylation of pyruvate via pyruvate carboxylase. This is also reflected in the isotopologue pattern of aspartate, where we found fractions of M+1, M+2 and M+4 as a result of one or more rounds of TCA cycle and also a fraction of M+3 derived directly from fully labelled pyruvate. Since DAP is synthesized from aspartate and pyruvate, the pattern of DAP also showed a large fraction of M+3, again derived from fully labelled pyruvate. The other fractions resulted from differentially labelled pyruvate and aspartate. Also, a small fraction of M+7 was found, derived from fully labelled aspartate and fully labelled pyruvate. Lysine is made by a decarboxylation of DAP, and therefore, all fractions except M+7 were also found in the isotopologue pattern of lysine (Figure S4C).

The isotopologue pattern of glutamate as a derivative of α-ketoglutarate was different from the pattern of glutamate in the time series experiments with ^{13}C-glucose, since in addition to M+1 and M+2, also M+3, M+4 and M+5 label was found. This could be explained by the high flux of serine into acetyl-CoA and then into the TCA cycle. Proline is made directly from glutamate, and therefore, the isotopologue pattern of proline was almost identical to that of glutamate. Proline (but not glutamate) was also a component of the growth medium, and ^{13}C-enrichment in proline was detected only after 36 h (4.70%). This finding is in agreement with

the notion that proline from the medium was consumed at that time and had to be synthesized *de novo* by *L. pneumophila* (Figure 3C, Figure S4C).

Finally, upon incubation with [U-$^{13}C_3$]serine as precursor also histidine and mannose were found to be highly ^{13}C-enriched (55.88% and 40.40% after 48 h), although also unlabelled glucose and glycerol were present in the medium. Mannose showed the same isotopologue pattern as in the labelling experiments with ^{13}C-glucose being mostly M+3 and M+6 labelled. Histidine on the other hand also had a larger M+6 fraction derived from fully labelled ribose via the PPP and a ^{13}C-labelled atom from ATP that is finally transferred onto the PRPP unit in the course of this biosynthetic pathway (Figure 3C, Figure 3D; Figure S4C).

Carbon flux of substrates into different metabolic markers

For an overview of the time-dependent metabolism of glycerol, glucose and serine by *L. pneumophila* in CE MDM, we chose four metabolites that are characteristic for different metabolic pathways and not present in the medium, so that they had to be synthesized *de novo* by the bacteria. Thus, the overall ^{13}C-excess of alanine (from pyruvate), histidine (through PPP), DAP (through the TCA cycle and from pyruvate) and PHB (from acetyl-CoA) was followed over time in the period of 12 h – 48 h (Figure 4).

When grown with ^{13}C-glycerol as precursor, only histidine showed high ^{13}C-abundances and only after 36 h and 48 h growth (Figure 4A). In time series with ^{13}C-glucose, histidine also showed by far the highest ^{13}C-enrichment of the four metabolites. However, significant enrichment in histidine was found already after 12 h of growth. Also the overall enrichment in all metabolites was higher compared with ^{13}C-glycerol as precursor, and it increased continuously over the entire time course (Figure 4B). When fed with ^{13}C-serine, the overall enrichment peaked after 24 h and dropped afterwards for all metabolites. In general, the overall enrichment was much higher in this case compared with glycerol or glucose as precursor, and alanine was the highest labelled metabolite (Figure 4C). Taken together, these

findings illustrate how different carbon sources are used in specific ways by *L. pneumophila*. Serine serves as an effective carbon source that is metabolized during all growth phases, while glycerol does not seem to be used during the exponential but only in the stationary growth phase. The same holds true for glucose, although this compound is already partly shuffled into the PPP during earlier growth phases, providing the precursors for histidine.

To illustrate the different carbon flow from glycerol, glucose and serine, we calculated the ratio of ^{13}C-excess in histidine and alanine and plotted it against time (Figure 4D). These amino acids were chosen as markers for different metabolic pathways: alanine as marker for carbon flux directed towards the TCA cycle and histidine for the PPP. Thus, the ratio between these amino acids shows how a carbon source is preferentially used. A high ratio value indicates a strong carbon flux into the PPP, while a small value indicates preferential flow into the TCA cycle. With ^{13}C-serine as a precursor, the ratio always stayed below 1, indicating that the main carbon flow was directed into the TCA cycle. In contrast, when fed with ^{13}C-glycerol or ^{13}C-glucose, the ratio was high, reaching a value of 5 after 36 h, demonstrating that the carbon flow was mainly directed to the PPP. Glycerol was only used after 36 h of growth, and incorporation into alanine and histidine was not significant at earlier time points, resulting in a low ratio of histidine to alanine. However, this is a mere result of the low overall ^{13}C-excesses in histidine and alanine and does not indicate that the carbon flow was directed towards the TCA cycle (Figure 4D). In summary, these results clearly show that serine is used as a major carbon source by *L. pneumophila* and carbon flow from serine is mainly directed towards the TCA cycle, while glucose and especially glycerol are not used as effectively as serine and carbon flow from these compounds is preferentially directed towards gluconeogenesis and the PPP.

Intracellular production of mannose by L. pneumophila *growing in* A. castellanii

To analyse the role and fate of different substrates during intracellular growth of *L. pneumophila*, we performed *in vivo* growth assays with *A. castellanii*. To this end, we infected *A. castellanii* with either *L. pneumophila* wild-type or the mutant strain Δ*glpD*. The infected amoeba were washed and incubated in Ac buffer, which does not contain any nutrients. Immediately after infection, more than 90% of the bacteria localized intracellularly (Figure S5; data not shown). 5 h post infection, ^{13}C-glycerol, ^{13}C-glucose or ^{13}C-serine was added to the infected amoeba and it was assessed whether the compounds affect the growth of *L. pneumophila* residing in the LCV and how they are metabolized. The infection was stopped before the bacteria could lyse the LCV or the host cell to prevent contact of the bacteria with labelled substrate in the extracellular milieu. This was tested by microscopy, before the samples were further processed.

At 15 h post infection, the infected amoeba were lysed and eukaryotic cell debris and bacteria were separated using an established protocol (Schunder *et al.*, 2014). This procedure yielded 3 fractions, containing eukaryotic components (F1), *L. pneumophila* bacteria (F2) or soluble proteins/factors (F3). ^{13}C-Excess and isotopologue profiles of amino acids, DAP, PHB and mannose from all fractions were measured. As ^{13}C-excess and isotopologue profiles in the fractions F1 and F3 were always identical (data not shown), we focussed only on F1 and F2. Furthermore, to rule out possible bacterial cross contamination in F1, samples were always visually inspected by microscopy, and aliquots were plated on CYE agar. As an internal control, we also monitored the amount of DAP in F1 and F2, as DAP is a cell wall component specific for bacteria. The amount of DAP in fraction F1 did never exceed 10%, so we concluded that bacterial contamination in F1 was always below 10%. Lastly, we also used uninfected amoeba fed either with ^{13}C-glycerol, ^{13}C-glucose or ^{13}C-serine to assess the influence of *L. pneumophila* infection on the metabolism of the amoeba. ^{13}C-Excess and isotopologue profiles of all *in vivo* experiments are documented in Table S5.

Uninfected *A. castellanii* incorporated ^{13}C-glycerol very efficiently into the amino acids alanine, aspartate, glutamate, glycine and serine, indicating that glycerol is a good carbon substrate for *A. castellanii*. Upon infection with *L. pneumophila* wild-type or Δ*glpD*, the incorporation of label into amino acids was completely abolished (Figure S6A, F1). Also, in the fraction F2 containing *L. pneumophila* wild-type or Δ*glpD*, no significant incorporation of ^{13}C-label into any of the measured amino acids was detectable.

The bacterial fraction F2 of ^{13}C-glycerol-fed amoeba infected with wild-type *L. pneumophila* yielded significant label in mannose (Figure 5A). Substantially less mannose was labelled in fraction F1 of wild-type-infected or in F1 and F2 of Δ*glpD*-infected *A. castellanii*. The isotopologue profile of mannose in fraction F2 of amoeba infected with wild-type *L. pneumophila* revealed that the sugar was mostly M+3 labelled (Figure 5D). This result is in line with our *in vitro* experiments, suggesting that also *in vivo* glycerol was used in gluconeogenesis for the production of hexoses. Moreover, the fact that no label was found in the Δ*glpD* mutant indicates that incorporation of ^{13}C-label into mannose in wild-type bacteria was a result of the direct uptake of glycerol into the LCV and the synthesis of mannose from glycerol by *L. pneumophila* via the glycerol-3-phosphate dehydrogenase GlpD (Figure 5A).

^{13}C-Glucose was also efficiently metabolized by uninfected *A. castellanii,* as already observed in previous studies (Schunder *et al.*, 2014). Again, an infection with wild-type *L. pneumophila* resulted in a significant drop in ^{13}C-incorporation in fraction F1. In contrast, the bacterial fraction F2 yielded significant ^{13}C-label in alanine, glutamate, DAP and PHB (Figure S6B). Notably, fraction F1 of wild-type-infected amoeba showed only minor ^{13}C-enrichment in mannose, while this carbohydrate was highly enriched in the bacterial fraction F2 (4.47%) (Figure 5B). The isotopologue pattern of mannose in F2 was characterized by M+3 and M+6 labels (Figure 5D), and therefore, almost identical to *L. pneumophila* grown in MDM. These results indicate that also glucose was taken up directly from the host (M+6) and metabolized by the bacteria. The M+3 label reflects glycolytic cycling via glycolysis and/or

the ED pathway, followed by gluconeogenesis and/or the PPP using a $^{13}C_3$-triose phosphate unit and an unlabelled substrate in the assembly process.

Finally, ^{13}C-serine was not as efficiently metabolized by uninfected amoeba as glucose and glycerol, since ^{13}C-incorporation was observed only in serine and its direct derivative glycine. Significantly more ^{13}C-incorporation was detected in fraction F1 of *A. castellanii* infected with wild-type *L. pneumophila*. However, the highest values of label from [U-$^{13}C_3$]serine were observed in F2, especially in alanine, serine, DAP and PHB (Figure S6C), in agreement with earlier observations (Schunder *et al.*, 2014). Interestingly, absolutely no incorporation occurred into mannose neither in F1 nor in F2, indicating that serine was not used for synthesis of this hexose by *L. pneumophila* or *A. castellanii*, respectively (Figure 5C). Notably, in all *in vivo* experiments, no label occurred in histidine, suggesting that this amino acid was efficiently taken up from the host cell and not synthesised *de novo* by *L. pneumophila* growing intracellularly.

Taken together, the data show that glycerol and glucose were taken up by *A. castellanii*, transported to the LCV predominantly without being metabolized and then directly utilized by *L. pneumophila*. Using this experimental setup, we proved that *L. pneumophila* also uses glycerol intracellularly as a substrate and exclusively in anabolic reactions, as shown in MDM minimal growth medium. The absence of label in mannose, when fed with ^{13}C-serine, suggests that similar to growth *in vitro* (Figure 4), *L. pneumophila* growing *in vivo* preferentially directs the flow of carbon from different substrates to distinct metabolic branches.

Discussion

Using genetic and biochemical approaches we show in this study that *L. pneumophila* catabolizes glycerol under extra- and intracellular conditions. To our knowledge this is the first study to show the direct usage of glycerol (or glucose) by intracellularly growing *L.*

pneumophila. The Δ*glpD* mutant showed a replication and competition defect compared with wild-type *L. pneumophila*, suggesting that glycerol might be used as an intracellular carbon source by the bacteria. In agreement with this notion, the *gpsA* gene encoding glycerol-3-phosphate dehydrogenase in *Legionella oakridgensis*, was recently identified as a virulence factor using *Acanthamoeba lenticulata* as a host (Brzuszkiewicz *et al.*, 2013).

Isotopologue profiling of *L. pneumophila* grown in MDM with [U-$^{13}C_3$]glycerol revealed carbon flux from glycerol through gluconeogenesis (for the production of mannose) and through the PPP (for the *de novo* synthesis of histidine). *L. pneumophila* metabolizes glucose preferentially via the ED pathway, and thus, the EMP pathway is not the preferred route for carbohydrate catabolism (Eylert *et al.*, 2010, Harada *et al.*, 2010). Our study now proves that the gluconeogenic pathway is active in *L. pneumophila*. A critical step in this pathway is the conversion of fructose-1,6 diphosphate to fructose-6 phosphate catalyzed by fructose 1,6-bisphosphatase. A corresponding homologue is not found in *Legionella* spp. genomes, and only phosphofructokinase (*lpg1913 alias pfkA*) is annotated (Chien *et al.*, 2004, Cazalet *et al.*, 2010). Yet, fructose-1,6-bisphosphatase activity in *L. pneumophila* cell extracts is tenfold higher than phosphofructokinase activity, indicating that this step in the EMP pathway favors the gluconeogenic rather than the glycolytic direction (Keen & Hoffman, 1984). Interestingly, the putative *L. pneumophila* phosphofructokinase is homologous to eukaryotic and bacterial PfkA enzymes that do not use ATP but pyrophosphate as cofactor and are reversible (Arimoto *et al.*, 2002, Costa dos Santos *et al.*, 2003). Thus, *L. pneumophila* PfkA might also catalyze both the forward (glycolytic) and the reverse (gluconeogenic) reaction.

Our data show for the first time activity of at least parts of the PPP in *L. pneumophila*. The genome of *L. pneumophila* encodes complete EMP and ED pathways, but only an incomplete PPP lacking the oxidative branch (6-phosphogluconate-dehydrogenase) and transaldolase (Cazalet *et al.*, 2004, Chien *et al.*, 2004). Accordingly, the key metabolite for entry into the PPP is likely fructose-6-phosphate rather than glucose-6-phosphate. The non-oxidative branch

of the PPP is essential for the conversion of carbohydrates. The C5-sugars required for the synthesis of histidine, purines and pyrimidines can be made directly from fructose-6-phosphate (together with glyceraldehyde-3-phosphate) in the transketolase reaction. Ribose-5-phosphate is then produced through reactions catalyzed by ribulose-5-phopsphate isomerase and epimerase. While the non-oxidative PPP branch is sufficient for the interconversion of sugars, it cannot provide $NADPH/H^+$. *L. pneumophila* can compensate the lack of the oxidative PPP branch by utilizing the ED pathway, which also generates $NADPH/H^+$.

Unexpectedly, when the *L. pneumophila* Δ*glpD* mutant strain was grown *in vitro* in the presence of ^{13}C-glycerol, lactate (but no other metabolites) showed some ^{13}C-enrichment. Lactate could be produced by a detoxification reaction of methylglyoxal, which is a byproduct of glycerol metabolism. Methylglyoxal can be generated non-enzymatically from glyceraldehyde-3-phosphate or dihydroxyacetone-phosphate in wild-type bacteria. As this route is blocked in the mutant lacking *glpD,* the bacteria might use glycerol dehydrogenase to make dihydroxyacetone, which is converted non-enzymatically to methylglyoxal. Since this intermediate is toxic, it is converted to lactate via the glyoxalase system (Figure S7) (Cooper, 1984, Riddle & Lorenz, 1973, Subedi *et al.*, 2008).

L. pneumophila utilized glycerol only in the stationary growth phase, while serine and (to a lower extent) glucose were metabolized already in early growth phases. The amount of ^{13}C-incorporation from these substrates indicates that serine is indeed the preferred carbon source for *L. pneumophila* as shown also in previous studies (Eylert *et al.*, 2010). ^{13}C-Incorporation from ^{13}C-labelled glucose was high (20.72 % in His after 48 h), while ^{13}C-incorporation from ^{13}C-glycerol was rather low (3.00 % in His after 48 h). These findings suggest that glycerol plays only a minor role for *L. pneumophila* in the hierarchy of carbon substrates, at least under extracellular conditions. The ratio of ^{13}C-excess, calculated from histidine as marker of the PPP and alanine as marker of the energy-generating lower part of glycolysis and the TCA cycle, showed that glycerol and glucose were predominantly used for gluconeogenesis and the

PPP, respectively, while serine was fed mainly into the lower part of the glycolytic pathway and the TCA cycle.

Based on these results, we propose a bipartite model for the metabolism of *L. pneumophila* (Figure 6). According to this model, the carbon metabolism of *L. pneumophila* can be divided into two modules: module 1, comprising the ED pathway, gluconeogenesis and the PPP, provides essentially $NADPH/H^+$ and the precursors for the anabolic, energy-consuming pathways, leading to cell wall components, nucleotides, histidine and aromatic amino acids, and module 2, comprising the lower part of the glycolytic pathway and the TCA cycle, which provides ATP, $NADH/H^+$, $FADH_2$ and the precursors for the biosynthesis of aliphatic amino acids and fatty acids/lipids. Module 1 is thus the energy-consuming part, essential for cell wall biosynthesis and hence cell division and proliferation, while module 2 is the major energy-generating part of the metabolism, which supplies ATP by substrate phosphorylation and by oxidative phosphorylation via $NADH/H^+$-dependent aerobic respiration. In *L. pneumophila*, the metabolic flow of glycerol and glucose is predominantly directed towards gluconeogenesis and PPP thus serving module 1, while serine is mainly used for energy-generating reactions and thus serves module 2 (Figure 6).

Noteworthy, our *in vivo* data also support a bipartite metabolism of intracellularly growing *L. pneumophila*. Addition of ^{13}C-glycerol to infected *A. castellanii* resulted in the exclusive incorporation of ^{13}C-label into mannose in the bacterial fraction. This was dependent on GlpD and did not occur in the host cell. Moreover, ^{13}C-glucose was also metabolized mainly to mannose by intracellular *L. pneumophila*. Interestingly, no ^{13}C-incorporation from ^{13}C-serine into mannose was detectable *in vivo*, neither in the host nor in intracellular *L. pneumophila*, while substantial incorporation was observed into amino acids, DAP and PHB.

A modular metabolism is also employed by other intracellular bacterial pathogens, and thus, seems to represent a general concept. However, depending on the microorganism, the same substrate might be metabolized by different modules. Other than *L. pneumophila*, *L.*

monocytogenes can grow on glycerol as sole carbon source *in vitro* (Schneebeli & Egli, 2013). Intracellularly, *L. monocytogenes* uses amino acids, glucose-6-phosphate and glycerol imported from the host cell (Grubmüller *et al.*, 2014). Yet, amino acids are not catabolized by *L. monocytogenes* but directly used for protein synthesis, while glycerol is efficiently used for energy generation, and glucose-6-phosphate predominantly serves anabolic purposes (Grubmüller *et al.*, 2014). Intracellularly growing *Mycobacterium tuberculosis* also employs a modular metabolism, such that acetate is employed for energy generation, while an unknown C_3 substrate is used for anabolic purposes and in the PPP (de Carvalho *et al.*, 2010). Furthermore, carbon flux from dextrose only occurs in the PPP, and the sugar is not used for energy generation. Under these conditions, *M. tuberculosis* also imports amino acids from the host, but uses these compounds only for protein synthesis (Beste *et al.*, 2013).

Since *L. pneumophila* seems to metabolize glycerol in later growth phases, a prominent source of intracellular glycerol might be the disintegration of host cell membranes upon LCV lysis through secreted phospholipases (Lang & Flieger, 2011). The finding that glycerol and glucose are directly metabolized by intracellular *L. pneumophila* suggests that the LCV is also accessible for substrates from the extracellular milieu of infected cells. Yet, the mode of uptake of these compounds into LCVs is unclear. Glycerol could enter the host cell via diffusion or transport. Aquaglyceroporines are common transporters in eukaryotes that facilitate uptake of water and glycerol and were also shown to be involved in innate immunity (Zhu *et al.*, 2011). Intracellularly growing *L. pneumophila* exploits host cell transporters to (Wieland *et al.*, 2005), and the proteome of purified LCVs revealed a large number of eukaryotic transporters (Hoffmann *et al.*, 2014a), including glucose transporters (Slc2a1, Slc2a6) and a glycerol transporter (Slc37a1). Thus, these transporters likely associate with the LCV membrane and facilitate the uptake of substrates into the pathogen compartment.

Phosphorylated carbon substrates might play an important role for the nutrition of *L. pneumophila*. In the genome of *L. pneumophila* only a glycerol-3-phosphate transporter

(GlpT) is annotated, suggesting that the bacteria transport glycerol-3-phosphate rather than glycerol, even though the growth of *L. pneumophila* in MDM was not enhanced by glycerol-3-phosphate (Figure 1C). The proteome of purified LCVs indicates that the eukaryotic glycerol kinase (Gk) might be associated with the LCV membrane (Hoffmann *et al.*, 2014a). This enzyme could phosphorylate cytoplasmic glycerol to glycerol-3-phosphate, which could be taken up into the LCV and subsequently transported into the bacteria. Isotopologue profiling experiments revealed that *L. pneumophila* growing extracellularly in presence of ^{13}C-glucose and unlabelled glucose-6-phosphate incorporated much less ^{13}C-label compared to ^{13}C-glucose alone (data not shown). Thus, intracellular *L. pneumophila* might also prefer glucose-6-phosphate as a growth substrate rather than glucose. To transport glucose-6-phosphate, the intracellular bacterium *Chlamydia pneumoniae* employs the transporter UhpC (*alias* HPTcp) (Schwoppe *et al.*, 2002), which also seems to be encoded in the *L. pneumophila* genome. Finally, *L. monocytogenes* also relies on glucose-6-phosphate rather than glucose for intracellular growth (Chico-Calero *et al.*, 2002, Grubmüller *et al.*, 2014).

L. pneumophila's metabolic strategy that relies on amino acids as substrates for energy production and uses carbohydrates mainly for anabolic purposes might put less nutritional stress on the host cell and therefore ensure successful infection and prolonged intracellular replication. Intracellular levels of glucose are a regulator of apoptosis in eukaryotes (Zhao *et al.*, 2008). As long as intracellular glucose levels are normal, anti-apoptotic proteins of the Bcl-2 family prevent cell death through apoptosis. The loss of glucose leads to decreased levels of Bcl-2 regulators (Alves *et al.*, 2006, Zhao *et al.*, 2007), which in consequence causes the activation of pro-apoptotic proteins (Chi *et al.*, 2000). Further studies are required to elucidate the intricate links between metabolism and virulence of *L. pneumophila*.

Experimental Procedures

Bacteria, cells and growth conditions

L. pneumophila strains (Table S1) were cultured under aerobic conditions at 37°C in AYE broth or grown on CYE agar plates supplemented with chloramphenicol (Cm; 5 μg mL^{-1}) or kanamycin (Km; 50 μg mL^{-1} in broth or 10 μg mL^{-1} in agar plates), if necessary. Alternatively, *L. pneumophila* was cultivated at 37°C in chemically defined medium (CDM) (Eylert *et al.*, 2010) modified from "Ristroph medium" (Ristroph *et al.*, 1981), minimal defined medium (MDM) (Table S2) or, in case of time series experiments, in MDM containing 50 mM glycerol and 11 mM glucose (carbon-enriched minimal defined medium; CE MDM) (Table S2). The media were prepared by dissolving all components except Fe-pyrophosphate in 950 ml ddH_20. The pH was adjusted to 6.3 (CDM) or 6.5 (MDM and CE MDM) using KOH, Fe-pyrophosphate was dissolved and filled up to 1 L.

Escherichia coli TOP10 was used for cloning and grown in LB medium at 37°C containing 30 μg mL^{-1} Cm or 50 μg mL^{-1} Km, if necessary. *A. castellanii (*ATCC 30234, lab collection) was grown in PYG medium at 23°C. Murine RAW264.7 macrophages (ATCC: TIB-71^{Tm}, lab collection) were cultivated in RPMI 1640 medium containing 10% heat inactivated fetal bovine serum and 2 mM glutamine at 37°C and 5% CO_2.

Construction of chromosomal deletion mutant strain

Chromosomal deletion of *glpD* in *L. pneumophila* wild-type JR32 was performed as described previously (Wiater *et al.*, 1994, Tiaden *et al.*, 2007), yielding strain CM01. The allelic exchange vector pCM018 (Table S1) was constructed in a four-way ligation using 0.8 kb of the 5′ and 0.8 kb of the 3′ flanking region of *glpD* and a Km resistance cassette from vector pUC4K. The flanking regions were amplified using the primer pairs glpD-LB-XbaI-fo, glpD-LB-SalI-re and glpD-RB-SalI-fo, glpD-RB-XbaI-re (Table S1), respectively, and digested using the restriction enzymes SalI and XbaI. The plasmid pUC4K was digested using SalI resulting in a 1.4 kB fragment containing the Km resistance cassette. The flanking regions and Km resistance cassette were then cloned into vector pLAW344 in a four-way ligation and

transformed into *E.coli* TOP10. Clones were analysed by restriction digestion and sequenced using the primers Kan2-fo and Kan2-re. *L. pneumophila* JR32 was transformed with pCM018 by electroporation. Km^R colonies were selected after 5 days growth at 30°C, grown overnight in AYE broth containing 50 µg mL^{-1} Km and then spotted on CYE/Km, CYE/Km/2% sucrose and CYE/Cm plates, and grown at 30°C to select for $Cm^S/Km^R/Suc^R$ colonies. Double-cross-over mutants were confirmed by PCR and sequenced. The *Legionella* homepage of the Pasteur Institute (http://genolist.pasteur.fr/Legiolist/) and the NCBI database (http://www.ncbi.nlm.nih.gov/) were used for sequence comparison.

The vector pCM021 (Table S1) for complementation of mutant strain CM01 was constructed using primer pair *glpD*-BamHI-fo-Kompl and *glpD*-SalI-re-Kompl. PCR products were digested using BamHI and SalI, cloned into vector pCR33 and transformed into *E. coli* TOP10. Cells were plated on LB/Cm plates, plasmids were re-isolated from single colonies, analysed by restriction digestion and sequenced.

Extracellular growth of L. pneumophila

To investigate the influence of glycerol on extracellular growing bacteria, *L. pneumophila* wild-type or Δ*glpD* were resuspended from CYE agar plates and grown in CDM overnight at 37°C (starting OD_{600} of 0.1) to an OD_{600} of maximum 1.0. Cultures were then diluted to OD_{600} = 0.1 in CDM or MDM with and without 50 mM glycerol or 50 mM glycerol-3-phosphate and further incubated for 48 h at 37°C. The optical density was assessed at several time points.

Intracellular replication of L. pneumophila

To analyse intracellular replication of *L. pneumophila*, we used previously published protocols (Harrison *et al.*, 2013). In brief, *A. castellanii* were grown in PYG medium, seeded in 96 well plates at 4 x 10^5 cells per well and incubated overnight at 23°C to allow replication

(doubling) of the amoeba. *L. pneumophila* strains harboring plasmid pNT-28 (constitutive GFP production) were resuspended from AYE plates in AYE/Cm (5µg ml^{-1}) and grown overnight at 37°C from a starting OD_{600} of 0.1 to an OD_{600} of 3. Bacteria were diluted in LoFlo medium (ForMedium), and amoeba were infected with *L. pneumophila* (MOI 20). Infections were synchronised by centrifugation at 500 × *g* for 10 min. 50 mM glycerol was added 4 h post infection to certain wells and infected amoeba were incubated at 30°C. GFP fluorescence was measured in a plate spectrophotometer (Optima FluoStar, BMG Labtech) at specific intervals. Murine RAW 264.7 macrophages were grown in RPMI medium containing 10% FBS and 2 mM glutamine at 37°C/5% CO_2. Infections were performed as described above for assays with *A. castellanii*, but the bacteria were diluted in RPMI 1640 medium prior to infection, and the plates were incubated at 37°C/5% CO_2. As the cell culture media used do not support growth of *L. pneumophila*, GFP fluorescence only reflects intracellular bacteria replication.

Intracellular growth of *L. pneumophila* was also assessed by determining cfu. To this end, *A. castellanii* or RAW 264.7 macrophages were suspended in Ac buffer [4 mM $MgSO_4$ × 7 H_2O, 0.4 mM $CaCl_2$, 3.4 mM sodium citrate dihydrate, 0.05 mM $Fe(NH_4)_2(SO_4)_2$ × 6 H_2O, 0.05 mM Na_2HPO_4 × 7 H_2O 2.5 mM KH_2PO_4, 0.05 mM NH_4Cl, pH 6.5] or RPMI 1640 medium respectively. 5×10^4 cells per well were seeded into 96-well plates and incubated at 23°C (amoeba) or 37°C and 5% CO_2 (macrophages) for 1 h. The cells were then infected with *L. pneumophila* (MOI 0.1), and the infection was synchronized by centrifugation at 500 × *g* for 10 min. The cells were further incubated for 1 h and washed with Ac buffer or RPMI 1640 medium. 50 mM glycerol was added 4 h post infection to certain wells. For complementation assays, the Δ*glpD* mutant strain harboring plasmid pCM021 was grown overnight with 1 mM IPTG to induce expression of *glpD*. Infection was performed as described above. After 48 h (macrophages) or 72 h (amoeba), the *L. pneumophila*-infected cells were lysed with 0.8% saponin, and appropriate dilutions were plated on CYE agar plates to determine cfu.

Intracellular growth of L. pneumophila *in competition assays*

For the competition assay, we used a previously published protocol (Kessler *et al.*, 2013). Briefly, *A. castellanii* (5×10^4 per well, 96-well plate) amoeba were infected at a 1:1 ratio with *L. pneumophila* wild-type and mutant strain Δ*glpD* (MOI 0.01 each) in Ac buffer. After centrifugation (500 × *g*, 10 min) and 1 h of infection, the amoeba were washed and fresh Ac buffer was added. The infection continued for 3 days at 37°C. After 3 days, the supernatant and lysed amoeba (0.8% saponin) were combined, diluted 1:1000 and used to infect fresh amoeba (5×10^4 per well, 96-well plate; 50 µl homogenate per 200 µl amoeba culture). Aliquots of the homogenates were plated in parallel on CYE agar plates with and without Km (10 µg mL^{-1}) to determine cfu and to distinguish between wild-type and Km-resistant mutants. Cells were then further incubated at 37°C for another 3 days, and lysis and reinfection was repeated. For complementation assays, the Δ*glpD* mutant harboring plasmid pCM021 was grown overnight with 1 mM IPTG to induce expression of *glpD*. *A. castellanii* were infected at a 1:1 ratio with wild-type *L. pneumophila* and Δ*glpD* harboring pCM021 (MOI 0.1 each) as described above. After 1, 2 and 3 days samples were taken as described above and aliquots were plated in parallel on CYE agar plates with and without Km (10 µg/mL).

Labelling of extracellular growing L. pneumophila

For isotopologue profiling, *L. pneumophila* wild-type and mutant Δ*glpD* were grown overnight in CDM (starting OD_{600} = 0.1). The next day, bacteria were diluted to an OD_{600} of 0.1 in 100 mL MDM containing 50 mM [U-$^{13}C_3$]glycerol and incubated in a shaking incubator at 180 rpm and 37°C for 48 h. The cells were harvested by centrifugation at 3500 × *g* for 15 min at 4°C and washed three times with cold Ac buffer (2 × 50 mL, 1 × 1 mL). An aliquot was plated on CYE agar plates. The resulting bacterial cell pellet was autoclaved at 120°C for 20 min, freeze-dried and then stored at -20°C until analysis.

For time course experiments, an overnight culture of *L. pneumophila* wild-type grown in CDM was diluted in CE MDM to a starting OD_{600} of 0.1. The CE MDM contained either 50 mM [U-$^{13}C_3$]glycerol, 11 mM [U-$^{13}C_6$]glucose or 6 mM [U-$^{13}C_3$]serine as a labelled substrate. Bacteria were cultivated in a shaking incubator at 180 rpm and 37°C. 30 mL samples were taken after 12 h, 24 h, 36 h and 48 h, OD_{600} was determined, and an aliquot was plated on CYE agar plates. Cells were harvested as described above.

Labelling of L. pneumophila *growing in* A. castellanii

To label intracellular growing *L. pneumophila* with ^{13}C-substrates, we used previously published protocols with minor modifications (Heuner & Eisenreich, 2013). In brief, *A. castellanii* was cultivated in 8 T75 cell culture flasks per bacterial strain (10 mL PYG/75cm^2 flask). After the cells reached confluency (~2 × 10^7 cells per flask), the amoeba were infected with *L. pneumophila* wild-type or Δ*glpD* (MOI 50), by adding bacteria grown in AYE to an OD_{600} of 3 at appropriate dilutions. The flasks were then centrifuged to synchronize infection (500 × *g*, 10 min) and incubated for 1 h at 37°C. To remove extracellular bacteria, cells were washed once with 10 mL pre-warmed Ac buffer, overlaid with 10 mL pre-warmed Ac buffer and further incubated at 37°C. 5 h post infection, either 50 mM [U-$^{13}C_3$]glycerol, 11 mM [U-$^{13}C_6$]glucose or 6 mM [U-$^{13}C_3$]serine was added to the flasks, and the cells were further incubated for 10 h. To determine the portion of extracellular *L. pneumophila*, the infected amoeba were washed as described above, spun onto microscopy slides, fixed with PFA, and extracellular bacteria were stained with a rabbit polyclonal FITC-conjugated anti-*L. pneumophila* antibody (Thermo Scientific; 1:50 in 5% FCS/Ac buffer, 1 h room temperature).

15 h post infection the amoeba were detached using a cell scraper, transferred into 50 mL reaction tubes, frozen at -80°C for 1 h and again thawed to room temperature. The suspension was then centrifuged at 200 × *g* for 10 min at 4°C, and the supernatant was transferred to new

50 mL reaction tubes. The pellet, representing eukaryotic cell debris (F1) was washed twice with 50 mL and once with 1 mL cold Ac buffer. The supernatant harvested after the first centrifugation step contained *L. pneumophila* bacteria (F2). This fraction was centrifuged at 3500 × *g* for 15 min at 4°C, and the resulting pellet was washed twice with 50 mL and once with 1 mL cold Ac buffer. The supernatant of F2 was filtered through a 0.22 µm pore filter to remove bacteria, and then 100% trichloroacetic acid was added to a final concentration of 10%. The supernatant was incubated on ice for 1 h and centrifuged at 4600 × *g* for 30 min at 4°C. The resulting pellet (F3) contained cytosolic proteins of *A. castellanii*. The pellets of F1, F2 and F3 were autoclaved at 120°C for 20 min, freeze-dried and stored at -20°C until analysis. To monitor cell lysis and the purity of F1 and F2, samples were analyzed by microscopy, and aliquots were plated on CYE agar plates.

Sample preparation of protein-derived amino acids, DAP and PHB

For isotopologue profiling of amino acids, diaminopimelic acid (DAP) and polyhydroxybutyrate (PHB), bacterial cells (approximately 10^9) or 1 mg of the freeze-dried host protein fraction were hydrolyzed in 0.5 mL of 6 M HCl for 24 h at 105°C, as described earlier (Eylert *et al.*, 2010). The HCl was removed under a stream of nitrogen, and the remainder was dissolved in 200 µL acetic acid. The sample was purified on a cation exchange column of Dowex 50Wx8 (H^+ form, 200-400 mesh, 5 × 10 mm), which was washed previously with 1 mL methanol and 1 mL ultrapure water. The column was eluted with 2 mL distilled water (eluate 1) and 1 mL 4 M ammonium hydroxide (eluate 2). An aliquot of the respective eluates was dried under a stream of nitrogen at 70°C.

The dried remainder of eluate 2 was dissolved in 50 µL dry acetonitrile and 50 µL *N*-(tert-butyldimethyl-silyl)-*N*-methyl-trifluoroacetamide containing 1% tert-butyl-dimethyl-silylchlorid (Sigma) and kept at 70°C for 30 min. The resulting mixture of tert-butyl-dimethylsilyl derivates (TBDMS) of amino acids and DAP was used for further GC/MS

analysis. Due to acid degradation, the amino acids tryptophan and cysteine could not be detected with this method. Furthermore, the hydrolysis condition led to the conversion of glutamine and asparagine to glutamate and aspartate. PHB was hydrolyzed to its monomeric component 3-hydroxybutyric acid. For derivatization of 3-hydroxybutyric acid, the dried aliquot of eluate 1 was dissolved in 100 µL *N*-methyl-*N*-(trimethylsilyl)-trifluoroacetamide (Sigma) and incubated in a shaking incubator at 110 rpm (30 min, 40°C). The resulting trimethylsilyl derivative (TMS) of 3-hydroxybutyric acid derived from PHB was used for GC/MS analysis without further treatment.

Sample preparation of methanol soluble metabolites including fatty acids

For isotopologue profiling of methanol soluble metabolites, 5 mg of the freeze-dried bacterial cells were mixed with 0.8 g of glass beads (0.25-0.05 mm) and 1 mL cooled 100% methanol. The mechanical cell lysis was performed for 3 × 20 s at 6.5 m/s using a ribolyser (Hybaid). After centrifugation at 2300 × *g* for 10 min, the supernatant was dried under a stream of nitrogen. The residue was dissolved in 50 µL dry acetonitrile and 50 µL *N*-(tert-butyldimethyl-silyl)-*N*-methyl-trifluoroacetamide containing 1% tert-butyl-dimethyl-silylchlorid (Sigma) and kept at 70°C for 30 min. The resulting mixture of tert-butyl-dimethylsilyl derivates (TBDMS) of polar metabolites and fatty acids was used for GC/MS analysis without further treatment.

Sample preparation of mannose

For isotopologue profiling of mannose, 5 mg of the freeze-dried bacterial cells were dissolved in 0.5 mL 3 M methanolic HCl and kept at 80°C overnight. After cooling to room temperature, the supernatant was dried under a stream of nitrogen. For derivatization, the residue was dissolved in 1 mL acetone containing 20 µL concentrated H_2SO_4 and kept at room temperature for 1 h. After addition of 2 mL saturated NaCl solution and 2 mL saturated

Na_2CO_3 solution the mixture was extracted twice with 3 mL ethyl acetate. The organic phases were combined and dried under a stream of nitrogen. The residue was dissolved in a mixture of 100 µL ethyl acetate and 100 µL acetic anhydride and kept at 60°C overnight. The derivatization reagent was removed under a stream of nitrogen, and the sample was dissolved in 100 µL anhydrous ethyl acetate. The resulting mixture of diisopropylidene/acetate derivatives was used for further GC/MS analysis. Since this procedure leads to the dephosphorylation of sugar-phosphates, the mannose detected could also originate from mannose-6-phosphate and mannose-1-phosphate.

Gas chromatography/mass spectrometry and isotopologue analysis

GC/MS-analysis was performed with a QP2010 Plus gas chromatograph/mass spectrometer (Shimadzu) equipped with a fused silica capillary column (Equity TM-5; 30 m × 0.25 mm, 0.25 µm film thickness; SUPELCO) and a quadrupol detector working with electron impact ionization at 70 eV. A volume of 0.1 to 6 µL of the sample was injected in 1:5 split mode at an interface temperature of 260°C and a helium inlet pressure of 70 kPa. With a sampling rate of 0.5 s, selected ion monitoring was used. Data was collected using LabSolution software (Shimadzu). All samples were measured three times (technical replicates). ^{13}C-Excess values and isotopologue compositions were calculated as described before (Eylert *et al.*, 2008) including: (i) determination of the spectrum of unlabelled derivatized metabolites, (ii) determination of mass isotopologue distributions of labelled metabolites, and (iii) correction of ^{13}C-incorporation concerning the heavy isotopologue contributions due to the natural abundances in the derivatized metabolites.

For analysis of amino acids, the column was kept at 150°C for 3 min and then developed with a temperature gradient of 7°C min^{-1} to a final temperature of 280°C that was held for 3 min. The amino acids alanine (6.7 min), glycine (7.0 min), valine (8.5 min), leucine (9.1 min), isoleucine (9.5 min), proline (10.1 min), serine (13.2 min), phenylalanine

(14.5 min), aspartate (15.4 min), glutamate (16.8 min), lysine (18.1 min), histidine (20.4 min) and tyrosine (21.0 min) were detected, and isotopologue calculations were performed with m/z $[M-57]^+$ or m/z $[M-85]^+$.

For analysis of DAP, the column was developed at 280°C for 3 min and then with a temperature gradient of 10°C min^{-1} to a final temperature of 300°C that was held for 3 min. The TBDMS-derivative of DAP was detected at a retention time of 6.2 min, and isotopologue calculations were performed with m/z $[M-57]^+$. For the detection of 3-hydroxybutyric acid derived from PHB, the column was heated at 70°C for 3 min and then developed with a first temperature gradient of 10°C min^{-1} to a final temperature of 150°C. This was followed by a second temperature gradient of 50°C min^{-1} to a final temperature of 280°C, which was held for 3 min. The TMS-derivative of 3-hydroxybutyric acid, was detected at a retention time of 9.1 min, and isotopologue calculations were performed with m/z $[M-15]^+$.

For the analysis of methanol soluble metabolites, the column was heated at 100°C for 2 min and then developed with a first temperature gradient of 3°C min^{-1} to a final temperature of 234°C, a second temperature gradient of 1°C min^{-1} to a final temperature of 237°C, and a third temperature gradient of 3°C min^{-1} to a final temperature of 260°C. TBDMS-derivatives of lactate (17.8 min), 3-hydroxybutyric acid (21.6 min), succinic acid (27.5 min), fumaric acid (28.7 min), malic acid (39.1 min), palmitic acid (44.0 min), stearic acid (49.4 min) and citric acid (53.25 min) were detected, and isotopologue calculations were performed with m/z $[M-57]^+$.

For diisopropylidene/acetate derivatives of sugars, the column was heated at 150°C for 3 min and then developed with a first temperature gradient of 10°C min^{-1} to a final temperature of 220°C, and with a second temperature gradient of 50°C min^{-1} to a final temperature of 280°C, which was held for 3 min. Isotopologue calculations were performed with m/z 287 $[M-15]^+$, a fragment which still contains all C-atoms of mannose. Retention

times and mass fragments of derivatized metabolites that were used for all isotopologue calculations are documented in Table S3A.

Acknowledgements

Work in the group of H.H. was supported by the Swiss National Science Foundation (SNF; 31003A_153200), the German Research Foundation (DFG; SPP1316, SPP1617), and the Bundesministerium für Bildung und Forschung (BMBF) through the program Infect-ERA in the context of the EUGENPATH network (031A410A). W.E. received funding from the BMBF through Infect-ERA (EUGENPATH).

References

Alves, N.L., I.A. Derks, E. Berk, R. Spijker, R.A. van Lier & E. Eldering, (2006) The Noxa/Mcl-1 axis regulates susceptibility to apoptosis under glucose limitation in dividing T cells. *Immunity* **24**: 703-716.

Arimoto, T., T. Ansai, W. Yu, A.J. Turner & T. Takehara, (2002) Kinetic analysis of PPi-dependent phosphofructokinase from *Porphyromonas gingivalis*. *FEMS Microbiol Lett* **207**: 35-38.

Beste, D.J., K. Noh, S. Niedenfuhr, T.A. Mendum, N.D. Hawkins, J.L. Ward, M.H. Beale, W. Wiechert & J. McFadden, (2013) ^{13}C-flux spectral analysis of host-pathogen metabolism reveals a mixed diet for intracellular *Mycobacterium tuberculosis*. *Chem Biol* **20**: 1012-1021.

Brüggemann, H., A. Hagman, M. Jules, O. Sismeiro, M.A. Dillies, C. Gouyette, F. Kunst, M. Steinert, K. Heuner, J.Y. Coppee & C. Buchrieser, (2006) Virulence strategies for infecting phagocytes deduced from the in vivo transcriptional program of *Legionella pneumophila*. *Cell Microbiol* **8**: 1228-1240.

Brzuszkiewicz, E., T. Schulz, K. Rydzewski, R. Daniel, N. Gillmaier, C. Dittmann, G. Holland, E. Schunder, M. Lautner, W. Eisenreich, C. Lück & K. Heuner, (2013) *Legionella oakridgensis* ATCC 33761 genome sequence and phenotypic characterization reveals its replication capacity in amoebae. *Int J Med Microbiol* **303**: 514-528.

Byrne, B. & M.S. Swanson, (1998) Expression of *Legionella pneumophila* virulence traits in response to growth conditions. *Infect Immun* **66**: 3029-3034.

Cazalet, C., L. Gomez-Valero, C. Rusniok, M. Lomma, D. Dervins-Ravault, H.J. Newton, F.M. Sansom, S. Jarraud, N. Zidane, L. Ma, C. Bouchier, J. Etienne, E.L. Hartland & C. Buchrieser, (2010) Analysis of the *Legionella longbeachae* genome and transcriptome uncovers unique strategies to cause Legionnaires' disease. *PLoS Genetics* **6**: e1000851.

Cazalet, C., C. Rusniok, H. Brüggemann, N. Zidane, A. Magnier, L. Ma, M. Tichit, S. Jarraud, C. Bouchier, F. Vandenesch, F. Kunst, J. Etienne, P. Glaser & C. Buchrieser, (2004) Evidence in the *Legionella pneumophila* genome for exploitation of host cell functions and high genome plasticity. *Nat Genet* **36**: 1165-1173.

Chen, D.E., S. Podell, J.D. Sauer, M.S. Swanson & M.H. Saier, Jr., (2008) The phagosomal nutrient transporter (Pht) family. *Microbiology* **154**: 42-53.

Chi, M.M., J. Pingsterhaus, M. Carayannopoulos & K.H. Moley, (2000) Decreased glucose transporter expression triggers BAX-dependent apoptosis in the murine blastocyst. *J Biol Chem* **275**: 40252-40257.

Chico-Calero, I., M. Suarez, B. Gonzalez-Zorn, M. Scortti, J. Slaghuis, W. Goebel, J.A. Vazquez-Boland & C. European Listeria Genome, (2002) Hpt, a bacterial homolog of the microsomal glucose-6-phosphate translocase, mediates rapid intracellular proliferation in *Listeria*. *Proc Natl Acad Sci U S A* **99**: 431-436.

Chien, M., I. Morozova, S. Shi, H. Sheng, J. Chen, S.M. Gomez, G. Asamani, K. Hill, J. Nuara, M. Feder, J. Rineer, J.J. Greenberg, V. Steshenko, S.H. Park, B. Zhao, E. Teplitskaya, J.R. Edwards, S. Pampou, A. Georghiou, I.C. Chou, W. Iannuccilli, M.E. Ulz,

D.H. Kim, A. Geringer-Sameth, C. Goldsberry, P. Morozov, S.G. Fischer, G. Segal, X. Qu, A. Rzhetsky, P. Zhang, E. Cayanis, P.J. De Jong, J. Ju, S. Kalachikov, H.A. Shuman & J.J. Russo, (2004) The genomic sequence of the accidental pathogen *Legionella pneumophila*. *Science* **305**: 1966-1968.

Cooper, R.A., (1984) Metabolism of methylglyoxal in microorganisms. *Ann Rev Microbiol* **38**: 49-68.

Costa dos Santos, A., W. Seixas da-Silva, L. de Meis & A. Galina, (2003) Proton transport in maize tonoplasts supported by fructose-1,6-bisphosphate cleavage. Pyrophosphate-dependent phosphofructokinase as a pyrophosphate-regenerating system. *Plant Physiol* **133**: 885-892.

D'Auria, G., N. Jimenez-Hernandez, F. Peris-Bondia, A. Moya & A. Latorre, (2010) *Legionella pneumophila* pangenome reveals strain-specific virulence factors. *BMC genomics* **11**: 181.

de Carvalho, L.P., S.M. Fischer, J. Marrero, C. Nathan, S. Ehrt & K.Y. Rhee, (2010) Metabolomics of *Mycobacterium tuberculosis* reveals compartmentalized co-catabolism of carbon substrates. *Chem Biol* **17**: 1122-1131.

Eylert, E., V. Herrmann, M. Jules, N. Gillmaier, M. Lautner, C. Buchrieser, W. Eisenreich & K. Heuner, (2010) Isotopologue profiling of *Legionella pneumophila*: role of serine and glucose as carbon substrates. *J Biol Chem* **285**: 22232-22243.

Eylert, E., J. Schär, S. Mertins, R. Stoll, A. Bacher, W. Goebel & W. Eisenreich, (2008) Carbon metabolism of *Listeria monocytogenes* growing inside macrophages. *Mol Microbiol* **69**: 1008-1017.

Faucher, S.P., C.A. Mueller & H.A. Shuman, (2011) *Legionella pneumophila* transcriptome during intracellular multiplication in human macrophages. *Front Microbiol* **2**: 60.

Finsel, I. & H. Hilbi, (2015) Formation of a pathogen vacuole according to *Legionella pneumophila*: how to kill one bird with many stones. *Cell Microbiol* **17**: 935-950.

Finsel, I., C. Ragaz, C. Hoffmann, C.F. Harrison, S. Weber, V.A. van Rahden, L. Johannes & H. Hilbi, (2013) The *Legionella* effector RidL inhibits retrograde trafficking to promote intracellular replication. *Cell Host Microbe* **14**: 38-50.

Fonseca, M.V., J.D. Sauer, S. Crepin, B. Byrne & M.S. Swanson, (2014) The *phtC-phtD* locus equips *Legionella pneumophila* for thymidine salvage and replication in macrophages. *Infect Immun* **82**: 720-730.

Gillmaier, N., A. Gotz, A. Schulz, W. Eisenreich & W. Goebel, (2012) Metabolic responses of primary and transformed cells to intracellular *Listeria monocytogenes*. *PLoS One* **7**: e52378.

Grubmüller, S., K. Schauer, W. Goebel, T.M. Fuchs & W. Eisenreich, (2014) Analysis of carbon substrates used by *Listeria monocytogenes* during growth in J774A.1 macrophages suggests a bipartite intracellular metabolism. *Front Cell Infect Microbiol* **4**: 156.

Haneburger, I. & H. Hilbi, (2013) Phosphoinositide lipids and the *Legionella* pathogen vacuole. *Curr Top Microbiol Immunol* **376**: 155-173.

Harada, E., K. Iida, S. Shiota, H. Nakayama & S. Yoshida, (2010) Glucose metabolism in *Legionella pneumophila*: dependence on the Entner-Doudoroff pathway and connection with intracellular bacterial growth. *J Bacteriol* **192**: 2892-2899.

Harrison, C.F., S. Kicka, V. Trofimov, K. Berschl, H. Ouertatani-Sakouhi, N. Ackermann, C. Hedberg, P. Cosson, T. Soldati & H. Hilbi, (2013) Exploring anti-bacterial compounds against intracellular *Legionella*. *PLoS One* **8**: e74813.

Hartel, T., E. Eylert, C. Schulz, L. Petruschka, P. Gierok, S. Grubmüller, M. Lalk, W. Eisenreich & S. Hammerschmidt, (2012) Characterization of central carbon metabolism of *Streptococcus pneumoniae* by isotopologue profiling. *J Biol Chem* **287**: 4260-4274.

Heuner, K. & W. Eisenreich, (2013) The intracellular metabolism of *Legionella* by isotopologue profiling. *Methods Mol Biol* **954**: 163-181.

Hilbi, H. & A. Haas, (2012) Secretive bacterial pathogens and the secretory pathway. *Traffic* **13**: 1187-1197.

Hoffmann, C., I. Finsel, A. Otto, G. Pfaffinger, E. Rothmeier, M. Hecker, D. Becher & H. Hilbi, (2014a) Functional analysis of novel Rab GTPases identified in the proteome of purified *Legionella*-containing vacuoles from macrophages. *Cell Microbiol* **16**: 1034-1052.

Hoffmann, C., C.F. Harrison & H. Hilbi, (2014b) The natural alternative: protozoa as cellular models for *Legionella* infection. *Cell Microbiol* **16**: 15-26.

Hubber, A. & C.R. Roy, (2010) Modulation of host cell function by *Legionella pneumophila* type IV effectors. *Ann Rev Cell Dev Biol* **26**: 261-283.

Isberg, R.R., T.J. O'Connor & M. Heidtman, (2009) The *Legionella pneumophila* replication vacuole: making a cosy niche inside host cells. *Nat Rev Microbiol* **7**: 13-24.

Keen, M.G. & P.S. Hoffman, (1984) Metabolic pathways and nitrogen metabolism in *Legionella pneumophila*. *Curr Microbiol* **11**: 81-88.

Kessler, A., U. Schell, T. Sahr, A. Tiaden, C. Harrison, C. Buchrieser & H. Hilbi, (2013) The *Legionella pneumophila* orphan sensor kinase LqsT regulates competence and pathogen-host interactions as a component of the LAI-1 circuit. *Environ Microbiol* **15**: 646-662.

Kriegeskorte, A., S. Grubmüller, C. Huber, B.C. Kahl, C. von Eiff, R.A. Proctor, G. Peters, W. Eisenreich & K. Becker, (2014) *Staphylococcus aureus* small colony variants show common metabolic features in central metabolism irrespective of the underlying auxotrophism. *Front Cell Infect Microbiol* **4**: 141.

Lang, C. & A. Flieger, (2011) Characterisation of *Legionella pneumophila* phospholipases and their impact on host cells. *Eur J Cell Biol* **90**: 903-912.

Lomma, M., D. Dervins-Ravault, M. Rolando, T. Nora, H.J. Newton, F.M. Sansom, T. Sahr, L. Gomez-Valero, M. Jules, E.L. Hartland & C. Buchrieser, (2010) The *Legionella pneumophila* F-box protein Lpp2082 (AnkB) modulates ubiquitination of the host protein parvin B and promotes intracellular replication. *Cell Microbiol* **12**: 1272-1291.

Molofsky, A.B. & M.S. Swanson, (2004) Differentiate to thrive: lessons from the *Legionella pneumophila* life cycle. *Mol Microbiol* **53**: 29-40.

Pine, L., J.R. George, M.W. Reeves & W.K. Harrell, (1979) Development of a chemically defined liquid medium for growth of *Legionella pneumophila*. *J Clin Microbiol* **9**: 615-626.

Price, C.T., S. Al-Khodor, T. Al-Quadan, M. Santic, F. Habyarimana, A. Kalia & Y.A. Kwaik, (2009) Molecular mimicry by an F-box effector of *Legionella pneumophila* hijacks a conserved polyubiquitination machinery within macrophages and protozoa. *PLoS Pathog* **5**: e1000704.

Price, C.T., T. Al-Quadan, M. Santic, I. Rosenshine & Y. Abu Kwaik, (2011) Host proteasomal degradation generates amino acids essential for intracellular bacterial growth. *Science* **334**: 1553-1557.

Riddle, V.M. & F.W. Lorenz, (1973) Nonenzymic formation of toxic levels of methylglyoxal from glycerol and dihydroxyacetone in Ringer's phosphate suspensions of avian spermatozoa. *Biochem Biophys Res Commun* **50**: 27-34.

Ristroph, J.D., K.W. Hedlund & S. Gowda, (1981) Chemically defined medium for *Legionella pneumophila* growth. *J Clin Microbiol* **13**: 115-119.

Rothmeier, E., G. Pfaffinger, C. Hoffmann, C.F. Harrison, H. Grabmayr, U. Repnik, M. Hannemann, S. Wölke, A. Bausch, G. Griffiths, A. Müller-Taubenberger, A. Itzen & H. Hilbi, (2013) Activation of Ran GTPase by a *Legionella* effector promotes microtubule polymerization, pathogen vacuole motility and infection. *PLoS Pathog* **9**: e1003598.

Sauer, J.D., M.A. Bachman & M.S. Swanson, (2005) The phagosomal transporter A couples threonine acquisition to differentiation and replication of *Legionella pneumophila* in macrophages. *Proc Natl Acad Sci U S A* **102**: 9924-9929.

Schatschneider, S., C. Huber, H. Neuweger, T.F. Watt, A. Puhler, W. Eisenreich, C. Wittmann, K. Niehaus & F.J. Vorholter, (2014) Metabolic flux pattern of glucose

utilization by *Xanthomonas campestris* pv. *campestris*: prevalent role of the Entner-Doudoroff pathway and minor fluxes through the pentose phosphate pathway and glycolysis. *Mol Biosyst* **10**: 2663-2676.

Schneebeli, R. & T. Egli, (2013) A defined, glucose-limited mineral medium for the cultivation of *Listeria* spp. *Appl Environ Microbiol* **79**: 2503-2511.

Schunder, E., N. Gillmaier, E. Kutzner, W. Eisenreich, V. Herrmann, M. Lautner & K. Heuner, (2014) Amino acid uptake and metabolism of *Legionella pneumophila* hosted by *Acanthamoeba castellanii*. *J Biol Chem* **289**: 21040-21054.

Schwoppe, C., H.H. Winkler & H.E. Neuhaus, (2002) Properties of the glucose-6-phosphate transporter from *Chlamydia pneumoniae* (HPTcp) and the glucose-6-phosphate sensor from Escherichia coli (UhpC). *J Bacteriol* **184**: 2108-2115.

Sherwood, R.K. & C.R. Roy, (2013) A Rab-centric perspective of bacterial pathogen-occupied vacuoles. *Cell Host Microbe* **14**: 256-268.

Steeb, B., B. Claudi, N.A. Burton, P. Tienz, A. Schmidt, H. Farhan, A. Maze & D. Bumann, (2013) Parallel exploitation of diverse host nutrients enhances *Salmonella* virulence. *PLoS Pathog* **9**: e1003301.

Steinert, M. & K. Heuner, (2005) *Dictyostelium* as host model for pathogenesis. *Cell Microbiol* **7**: 307-314.

Subedi, K.P., I. Kim, J. Kim, B. Min & C. Park, (2008) Role of GldA in dihydroxyacetone and methylglyoxal metabolism of *Escherichia coli* K12. *FEMS Microbiol Lett* **279**: 180-187.

Tesh, M.J. & R.D. Miller, (1981) Amino acid requirements for *Legionella pneumophila* growth. *J Clin Microbiol* **13**: 865-869.

Tesh, M.J., S.A. Morse & R.D. Miller, (1983) Intermediary metabolism in *Legionella pneumophila*: utilization of amino acids and other compounds as energy sources. *J Bacteriol* **154**: 1104-1109.

Tiaden, A., T. Spirig, S.S. Weber, H. Brüggemann, R. Bosshard, C. Buchrieser & H. Hilbi, (2007) The *Legionella pneumophila* response regulator LqsR promotes host cell interactions as an element of the virulence regulatory network controlled by RpoS and LetA. *Cell Microbiol* **9**: 2903-2920.

Vorwerk, H., J. Mohr, C. Huber, O. Wensel, K. Schmidt-Hohagen, E. Gripp, C. Josenhans, D. Schomburg, W. Eisenreich & D. Hofreuter, (2014) Utilization of host-derived cysteine-containing peptides overcomes the restricted sulphur metabolism of *Campylobacter jejuni*. *Mol Microbiol* **93**: 1224-1245.

Weber, S., C.U. Stirnimann, M. Wieser, D. Frey, R. Meier, S. Engelhardt, X. Li, G. Capitani, R.A. Kammerer & H. Hilbi, (2014) A type IV translocated *Legionella* cysteine phytase counteracts intracellular growth restriction by phytate. *J Biol Chem* **289**: 34175-34188.

Wiater, L.A., A.B. Sadosky & H.A. Shuman, (1994) Mutagenesis of *Legionella pneumophila* using Tn*903*dll*lacZ*: identification of a growth-phase-regulated pigmentation gene. *Mol Microbiol* **11**: 641-653.

Wieland, H., S. Ullrich, F. Lang & B. Neumeister, (2005) Intracellular multiplication of *Legionella pneumophila* depends on host cell amino acid transporter SLC1A5. *Mol Microbiol* **55**: 1528-1537.

Zhao, Y., B.J. Altman, J.L. Coloff, C.E. Herman, S.R. Jacobs, H.L. Wieman, J.A. Wofford, L.N. Dimascio, O. Ilkayeva, A. Kelekar, T. Reya & J.C. Rathmell, (2007) Glycogen synthase kinase 3alpha and 3beta mediate a glucose-sensitive antiapoptotic signaling pathway to stabilize Mcl-1. *Mol Cell Biol* **27**: 4328-4339.

Zhao, Y., H.L. Wieman, S.R. Jacobs & J.C. Rathmell, (2008) Mechanisms and methods in glucose metabolism and cell death. *Methods Enzymol* **442**: 439-457.

Zhu, N., X. Feng, C. He, H. Gao, L. Yang, Q. Ma, L. Guo, Y. Qiao, H. Yang & T. Ma, (2011) Defective macrophage function in aquaporin-3 deficiency. *FASEB J* **25**: 4233-4239.

Figure legends

Figure 1. Glycerol promotes intracellular growth of *L. pneumophila*. Extracellular growth of *L. pneumophila* wild-type and mutant Δ*glpD* in (**A**) CDM or (**B**) MDM with and without 50 mM glycerol or (**C**) in MDM with and without 50 mM glycerol-3-phosphate. Optical density at 600 nm was determined at the time points indicated. (**D**) Murine RAW 264.7 macrophages were infected (MOI 20) with *L. pneumophila* wild-type or Δ*glpD* harboring pNT-28 (constitutive GFP production). Glycerol was added 4 h post infection, and replication was determined by fluorescence. (**E**) Macrophages were infected with *L. pneumophila* wild-type, Δ*glpD* or Δ*glpD* harboring pCR33 or pCM021 (MOI 0.1). Glycerol was added 4h post infection, and cfu were determined 2 days post infection (1 way ANOVA test with Dunett`s multiple comparison test: * < 0.05, *** < 0.0001). (**F**) *A. castellanii* amoeba were infected (MOI 20) with *L. pneumophila* wild-type or Δ*glpD* harboring pNT-28 (constitutive GFP production). Glycerol was added 4 h post infection, and replication was determined by fluorescence. (**G**) Competition defect of Δ*glpD*. *A. castellanii* were infected with *L. pneumophila* wild-type and Δ*glpD* at a 1:1 ratio (MOI 0.01 each). After 3 days, cells were lysed and bacteria were used to infect new amoeba. cfu were quantified by plating aliquots on CYE agar plates. (**H**) Complementation of Δ*glpD* competition defect. *A. castellanii* amoeba were infected with *L. pneumophila* wild-type and Δ*glpD* harboring pCM021 at a 1:1 ratio (MOI 0.1 each). After 1, 2 and 3 days, the infected cells were lysed, and cfu were quantified by plating aliquots on CYE agar plates. Mean and SD of triplicates are shown. Data are representative of three independent experiments.

Figure 2. Glycerol metabolism of *L. pneumophila* grown in MDM. (**A**) *L. pneumophila* wild-type and Δ*glpD* were grown in MDM with 50 mM [U-$^{13}C_3$]glycerol as precursor, and cells were harvested after 48 h. ^{13}C-excess (in mol% as color map) of protein-derived amino acids, diaminopimelic acid (DAP), polyhydroxybutyrate (PHB), methanol soluble metabolites

and mannose was quantified by isotopologue profiling. (**B**) The isotopologue pattern of histidine, mannose and lactate from *L. pneumophila* wild-type and Δ*glpD* was determined. The columns indicate the relative fraction (in %) of the ^{13}C-isotopologues (M+1 to M+6). Data shown are mean and SD from three independent experiments. For numerical values, see Supporting Information.

Figure 3. ^{13}C-excess in key metabolites of *L. pneumophila* grown with [U-$^{13}C_3$]glycerol, [U-$^{13}C_6$]glucose or [U-$^{13}C_3$]serine as precursors. *L. pneumophila* wild-type was grown in CE MDM with either (**A**) 50 mM [U-$^{13}C_3$]glycerol, (**B**) 11 mM [U-$^{13}C_6$]glucose or (**C**) 6 mM [U-$^{13}C_3$]serine as precursors in the medium. Samples were taken after 12 h, 24 h, 36 h and 48 h. ^{13}C-incorporation (**A-C**) into protein-derived amino acids, diaminopimelic acid (DAP) and polyhydroxybutyrate (PHB) for all time points and (**D**) into methanol-soluble metabolites and mannose after 48 h was quantified. Color map correlates to mean value and SD of three independent experiments. For numerical values, see Supporting Information.

Figure 4. Analysis of carbon flux from different substrates into metabolic markers. Incorporation of ^{13}C-label over time into alanine, histidine, DAP and PHB of *L. pneumophila* fed with (**A**) 50 mM [U-$^{13}C_3$]glycerol, (**B**) 11 mM [U-$^{13}C_6$]glucose or (**C**) 6 mM [U-$^{13}C_3$]serine as precursor. (**D**) Ratio of ^{13}C-excess in histidine to ^{13}C-excess in alanine with ^{13}C-glycerol, ^{13}C-glucose or ^{13}C-serine as substrate shows carbon fluxes into the TCA cycle or into gluconeogenesis/PPP.

Figure 5. Analysis of mannose from *L. pneumophila* grown in *A. castellanii*. *A. castellanii* amoeba were infected with either *L. pneumophila* wild-type or Δ*glpD* (MOI 50) and washed 1 h post infection to remove extracellular bacteria. 5 h post infection (**A**) 50 mM [U-$^{13}C_3$]glycerol, (**B**) 11 mM [U-$^{13}C_6$]glucose or (**C**) 6 mM [U-$^{13}C_3$]serine were added. 15 h post

infection, the cells were lysed and eukaryotic cell debris and bacteria were separated, resulting in fractions F1, containing eukaryotic cell debris and fraction F2, containing *L. pneumophila*. (**D**) ^{13}C-excess of mannose in F1 and F2 of wild-type- or Δ*glpD*-infected amoeba, fed with (**A**) [U-$^{13}C_3$]glycerol, (**B**) [U-$^{13}C_6$]glucose or (**C**) [U-$^{13}C_3$]serine were analyzed, and the isotopologue pattern of mannose from F2 of WT-infected amoeba fed with [U-$^{13}C_3$]glycerol or [U-$^{13}C_6$]glucose was determined. Mean and SD of two independent experiments are shown. For numerical values, see Supporting Information.

Figure 6. The bipartite metabolism of *L. pneumophila*. The metabolism of *L. pneumophila* is divided into two modules, containing the ED pathway, gluconeogenesis and the PPP (**red-blue rectangle**) in module 1 and the TCA cycle (**green cycle**) as well as amino acid and fatty acid synthesis in module 2. Thick colored arrows represent main routes of carbon flow from glucose (**blue**), glycerol (**red**) and serine (**green**). Metabolic flow of glucose and glycerol is mainly restricted to the upper part of metabolism (**module 1**), while serine is mainly used in the lower, energy-generating part of metabolism (**module 2**). While glycerol is exclusively used for gluconeogenesis and the PPP in module 1, glucose and serine are channeled through module 2 (**dotted blue arrow**) as well as module 1 (**dotted green arrow**), respectively. **Abbreviations:** 6-PG. 6-phosphogluconate; KDPG, 2-keto-3-desoxy-phosphogluconate; PPP, pentose phosphate pathway; PHB, poly-hydroxybutyrate; TCA, tricarboxylic acid cycle; α-KGA, α-ketoglutaric acid; DAP, diaminopimelic acid. **Genes:** *tktA*, transketolase; *rpe*, ribulose-5-phosphate-epimerase; *rpiA*, ribulose-5-phosphate-isomerase; *lpg1414*, glycerol kinase; *glpD*, glycerol-3-phosphate dehydrogenase.

Supporting Information

$^{13}C_6$]glucose or (**C**) 6 mM [U-$^{13}C_3$]serine. Relative fractions of isotopologues (mol%) of (**D**) amino acids, DAP and PHB, or (**E**) polar metabolites and mannose from *L. pneumophila* wild-type grown in CE MDM supplemented with either (**i**) 50 mM [U-$^{13}C_3$]glycerol, (**ii**) 11 mM [U-$^{13}C_6$]glucose or (**iii**) 6 mM [U-$^{13}C_3$]serine of 48 h time points from time series experiments. M+x represents the mass of the unlabelled metabolite plus x labelled ^{13}C-atoms. Mean and SD from three independent experiments are shown. (**F**) Ratio of ^{13}C-excess in histidine to ^{13}C-excess in alanine calculated from time series experiments with *L. pneumophila* wild-type grown in CE MDM with either 50 mM [U-$^{13}C_3$]glycerol, 11 mM [U-$^{13}C_6$]glucose or 6 mM [U-$^{13}C_3$]serine as precursor. The ratio of means from samples taken after 12 h, 24 h, 36 h or 48 h is shown. SD was calculated from the highest possible (+) and the lowest possible (-) value.

Table S5. Isotopologue profiling of *L. pneumophila*-infected *A. castellanii*. (**A**) ^{13}C-Excess (mol%) of alanine, aspartate, glutamate, glycine, serine, DAP, PHB and mannose from experiments with uninfected *A. castellanii* and amoeba infected with *L. pneumophila* wild-type or Δ*glpD*. Infections were supplemented with either (**i**) 50 mM [U-$^{13}C_3$]glycerol, (**ii**) 11 mM [U-$^{13}C_6$]glucose or (**iii**) 6 mM [U-$^{13}C_3$]serine 5 h post infection. Cells were lysed and fractionated 15 h post infection, resulting in fraction 1 (**F1**), containing eukaryotic cell debris and fraction 2 (**F2**), containing *L. pneumophila* bacteria. (**B**) Relative fraction of isotopologues in alanine, aspartate, glutamate, glycine, serine, DAP und PHB (mol%) of *in vivo* infection and separation experiments. *A. castellanii* amoeba were either fed with (**i**) 50 mM [U-$^{13}C_3$]glycerol, (**ii**) 11 mM [U-$^{13}C_6$]glucose or (**iii**) 6 mM [U-$^{13}C_3$]serine. M+x represents the mass of the unlabeled metabolite plus x labelled ^{13}C-atoms. Mean and standard deviation from two independent experiments are shown. (**C**) Relative fraction of isotopologues in mannose (mol%) from fraction 2 (F2) of *in vivo* infection and separation experiments. *A. castellanii* cells were either fed with (**i**) 50 mM [U-$^{13}C_3$]glycerol or (**ii**)

11 mM [U-$^{13}C_6$]glucose. M+x represents the mass of the unlabelled metabolite plus x labelled ^{13}C-atoms. Mean and SD from two independent experiments are shown.

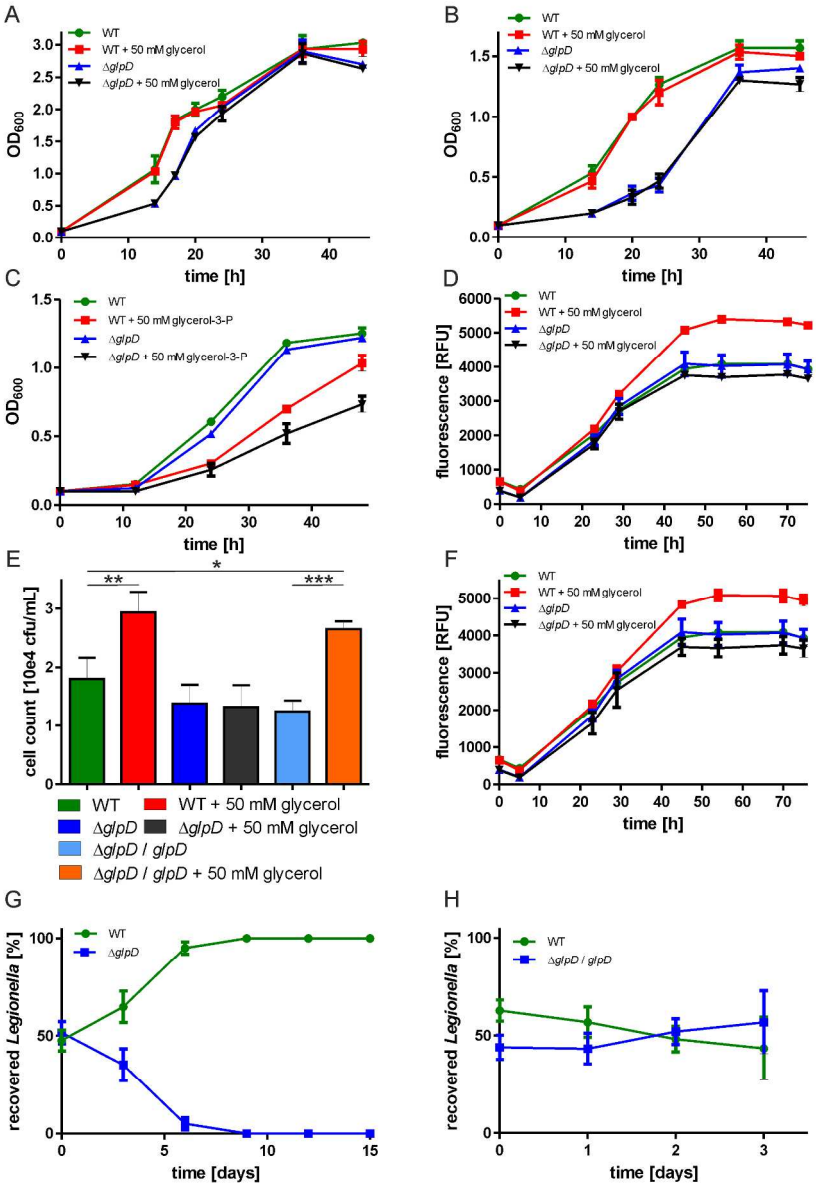

Figure 1
214x296mm (300 x 300 DPI)

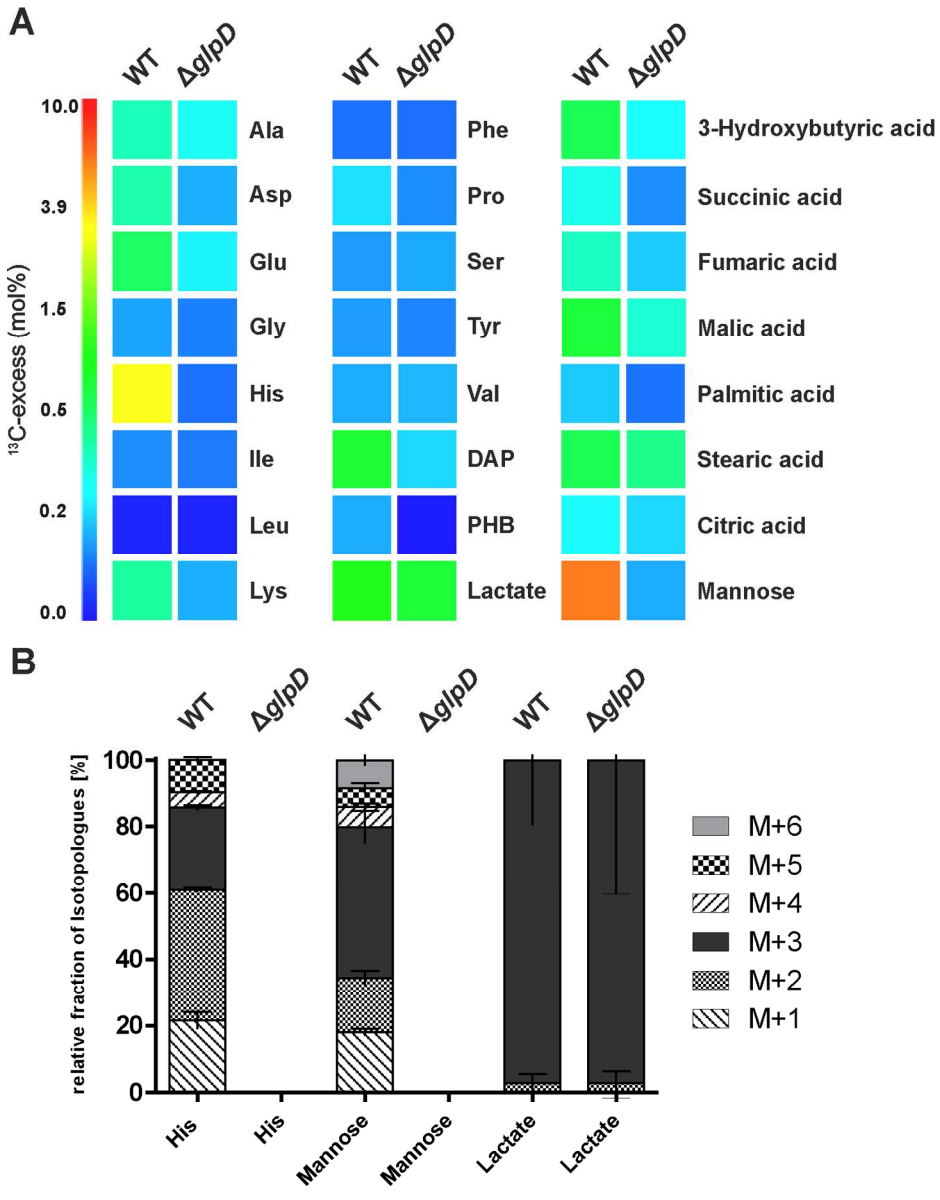

Figure 2
140x181mm (300 x 300 DPI)

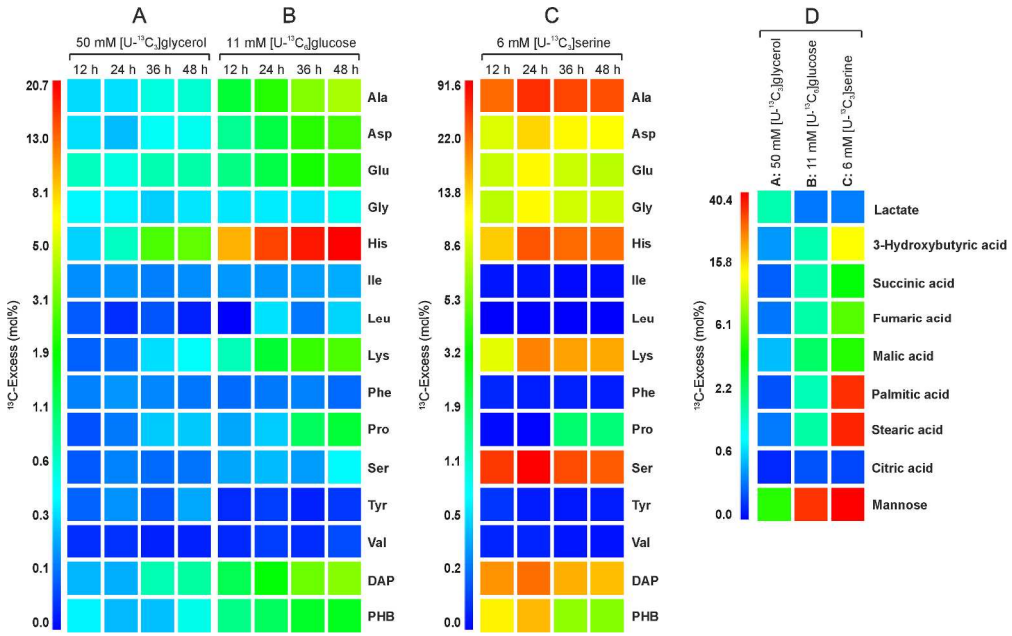

Figure 3
268x167mm (300 x 300 DPI)

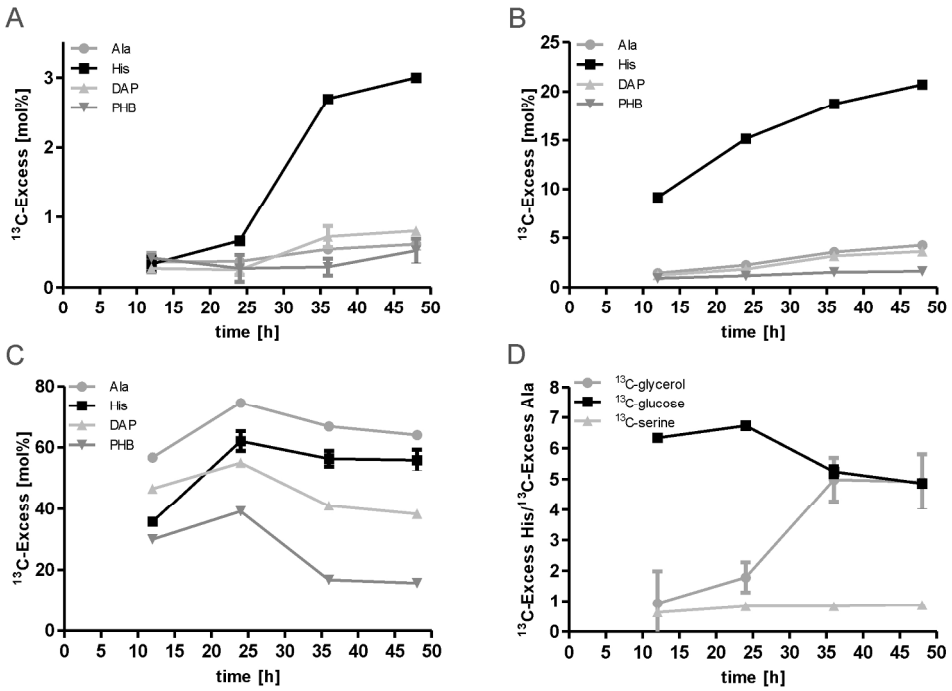

Figure 4
207x144mm (300 x 300 DPI)

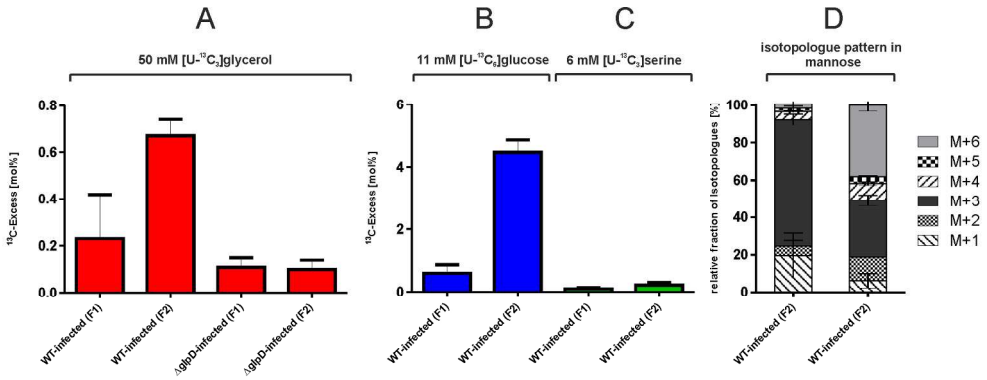

Figure 5
194x74mm (300 x 300 DPI)

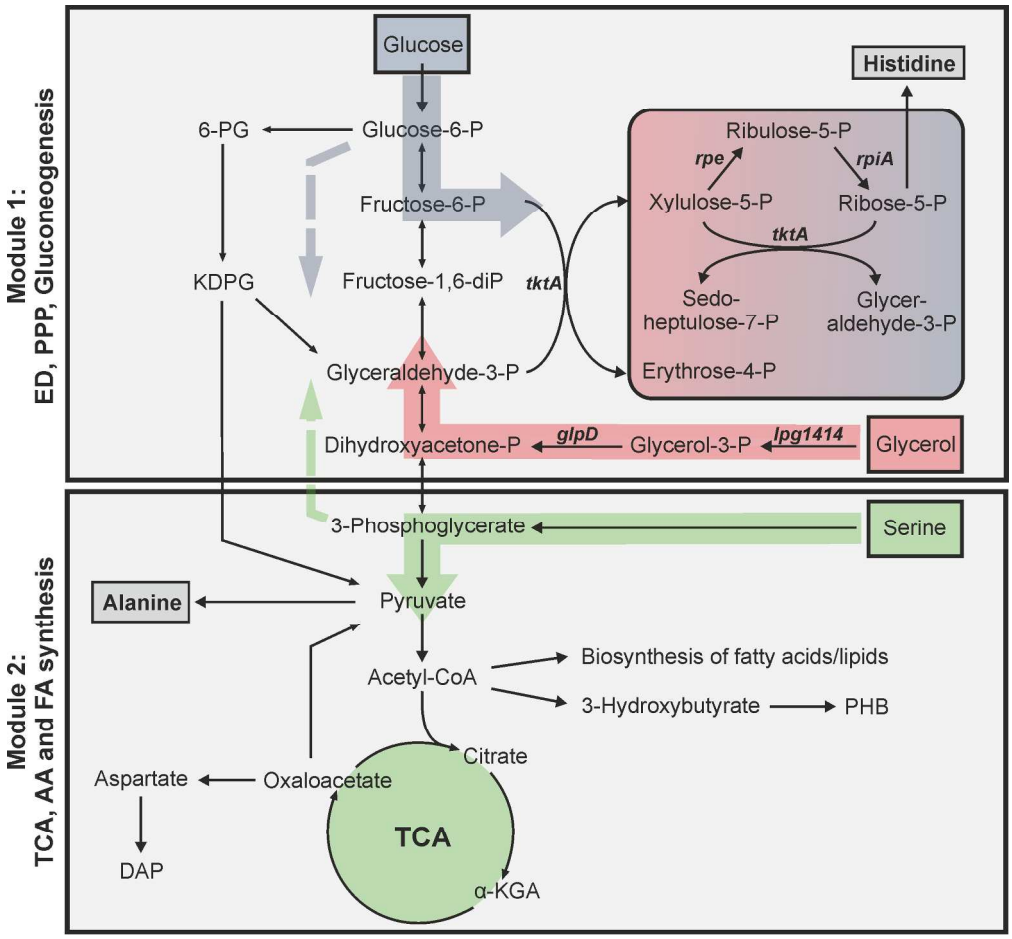

Figure 6
221x205mm (300 x 300 DPI)

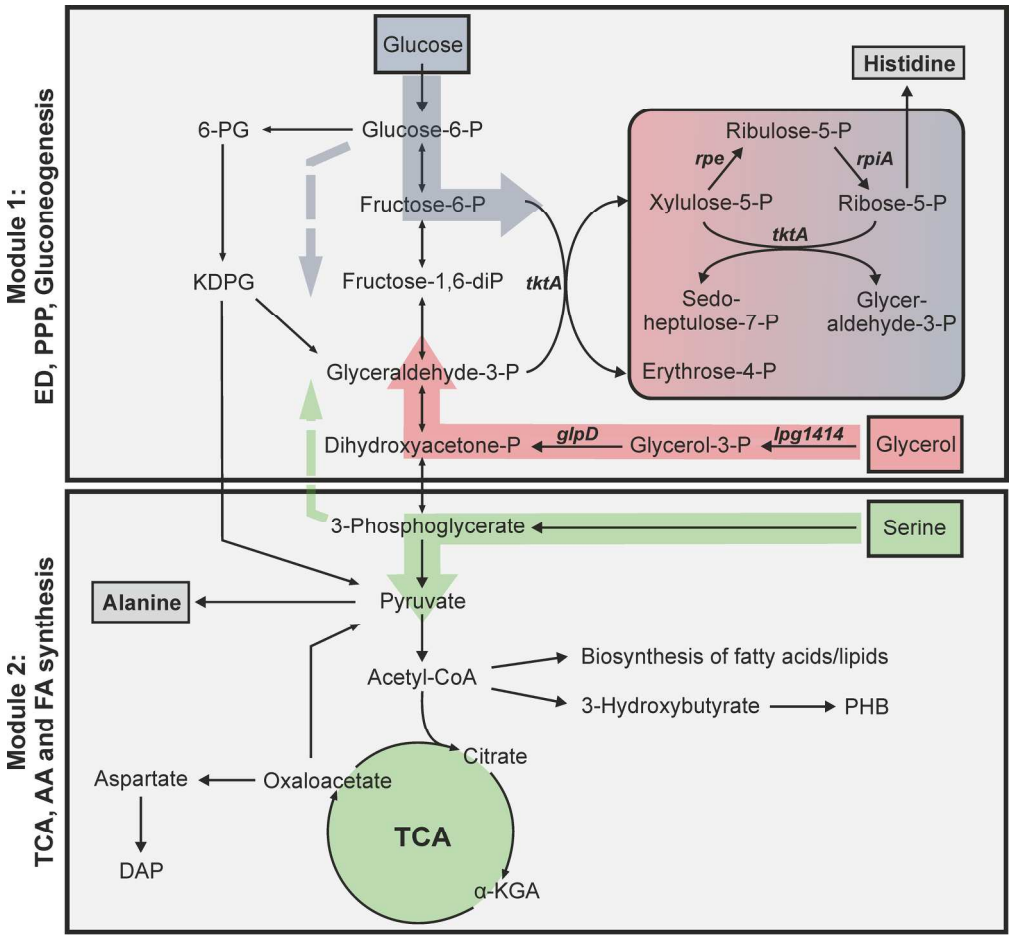

Graphical Abstract
205x190mm (300 x 300 DPI)

Abbreviated Summary

The facultative intracellular bacterium *Legionella pneumophila* causes the severe pneumonia Legionnaires´ disease. Extra- and intracellularly, *L. pneumophila* primarily metabolizes amino acids, but - as we show here by using a new defined growth medium and a method termed isotopologue profiling - also glycerol. The pathogen employs a bipartite metabolism, where glycerol and carbohydrates like glucose are mainly fed into energy-consuming synthetic processes, while amino acids such as serine serve as major energy supply.